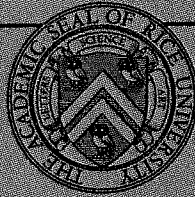


PRELIMINARY SCIENCE REPORT

Charged Particle Lunar
Environment Experiment
(CPLEE)



DEPARTMENT OF
SPACE SCIENCE



RICE UNIVERSITY
HOUSTON, TEXAS

PRELIMINARY SCIENCE REPORT

Charged Particle Lunar
Environment Experiment
(CPLEE)

by

Brian J. O'Brien
School of Physics
University of Sydney
Sydney, Australia

and

David L. Reasoner
Department of Space Science
Rice University
Houston, Texas

March, 1970

CHARGED PARTICLE LUNAR ENVIRONMENT EXPERIMENT

I. Introduction

A. Purpose of the Experiment

The primary scientific objective of the Charged Particle Lunar Environment Experiment (CPLEE) is to measure the fluxes of charged particles, electrons and ions, with energies ranging from 50 eV to 50,000 eV which bombard the lunar surface. These particles may result from a variety of phenomena, to wit:

1. Relatively stable plasma population in the geomagnetic tail including the so-called plasma sheet and neutral sheet.
2. Transient particle fluxes in the tail resulting from such phenomena as geomagnetic substorms and particle acceleration mechanisms similar to those which produce aurorae.
3. Plasma in the transition region between the geomagnetic tail and the shock front.
4. The solar wind, and particles resulting from the interaction between the solar wind and the lunar surface.
5. Solar cosmic rays, those particles thrown into interplanetary space by solar flare eruptions.
6. Photoelectrons at the lunar surface produced by the interaction of solar photons with the lunar surface material.
7. "Artificial events", for example particles produced by the impact of the Lunar Module.

Thus in one sense the moon serves as a satellite to carry the CPLEE instrument through various regions of space, and in another sense the CPLEE is a detector of phenomena resulting from the interaction of radiation with the lunar surface.

B. Summary of Observations

With the foregoing list of scientific objectives in mind, we report here the following preliminary observations.

1. Detection of stable, low-energy photoelectron fluxes at the lunar surface.
2. Observation of plasma clouds produced by the impact of the Apollo 14 Lunar Module ascent stage.
3. Observations of rapidly-fluctuating low-energy (50 - 200 eV) electrons in the magnetosheath and magnetotail.
4. Detection of fluxes of medium energy electrons with durations of a few minutes to some tens of minutes deep within the magnetotail.
5. Observation of electron spectra in the tail remarkably similar to electron spectra observed above terrestrial aurorae.
6. Observation of rapid time variations (10 sec) in solar wind fluxes observed in the magnetosheath and in interplanetary space.

II. Theoretical Basis

The original objectives of the Charged Particle Lunar Environment Experiment Subsystem, as outlined some five years ago, are still valid today. They are to measure the proton and electron fluxes at the lunar surface and to study their energy and angular distributions and their time variations. The results of these measurements will provide information on a variety of particle phenomena, important both in themselves and also for their relevance to lunar surface properties.

There is a category of radiation that may periodically envelop ALSEP at times of the full moon, when it is in the "magnetic tail" of the earth, which is swept downstream like a comet tail by the solar wind. We have speculated (O'Brien, 1967) that in this domain are accelerated the electrons and protons that cause auroras when they plunge into the terrestrial atmosphere. Indeed, it has been shown (e.g. Reasoner et al., 1968) that the ultimate source of auroral particles is the sun, and furthermore that an almost continuous replenishment of the magnetospheric particle population is necessary to sustain the observed auroral fluxes, (O'Brien, 1967).

The mechanisms which accelerate these particles to auroral energies are not understood, and simultaneous observations near the earth and near the moon are essential for detailed study of their general characteristics and morphology.

The solar wind may occasionally strike the surface of the moon. This "wind" is caused by the expansion into interplanetary space of the very hot outer envelope of the sun. The stream apparently carries energy and perturbations

towards the earth-moon system - and so it, the "solar wind", may be the source of energy that leads to such terrestrial phenomena as auroras and Van Allen radiation. Thus for this study the moon would serve as an excellent stable observation post in space.

However, apparently the pure interplanetary solar wind does not always hit the lunar surface (Lyon et al., 1967). Because the solar wind is supersonic and because the moon is sufficiently large to prove an obstacle to the flow of the wind, it is possible that at times there is a standing "shock" front. To date the only such phenomenon observed is caused by the terrestrial magnetic field which hollows out a cavity in the solar wind. The detailed physical processes that occur at such shock fronts are largely not understood, and they are of considerable fundamental interest in plasma research. If there is occasionally such a shock front near the moon, the CPLEE will observe the disordered (or thermalized) fluxes of electrons and protons which share energy on the downstream side of the shock. It appears, (Lyon et al., 1967) that the most usual situation is for a "shadowing" of the solar wind by the lunar surface, causing a plasma "void" on the dark side.

The instrument can also measure the lower-energy solar cosmic rays occasionally produced in solar eruptions or flares. To observe these low-energy particles one must place experimental packages beyond the reach of the modifying effects of an atmosphere and magnetic field such as the earth possesses. The moon is an excellent platform for such studies since both its atmosphere and magnetic field are so relatively negligible.

The sunlit lunar surface may be a veritable sea of low-energy photoelectrons generated by solar photons striking the surface (Walbridge, 1970). If such electrons are present, CPLEE will be in an excellent position to study them with its capability of detecting electrons with energies down to 40 eV. Studies of any such photoelectron layer are important in deducing surface properties related to photo-emission and gaining indirect information about lunar surface electric fields.

It should also be borne in mind that observations of the charged particle environment of the moon is of interest, not merely for its own sake, but because such particles affect the lunar environment. They may cause luminescence or coloration effects on the lunar surface. They may also sweep away a large proportion of the lunar atmosphere. Furthermore, they constitute a very important proportion of the electrical environment, and they may, for example, nullify electrostatic effects that would otherwise occur on the lunar surface.

III. Equipment

A. Description of the Instrument

CPLEE consists quite simply of a box supported by four legs. The box contains two similar physical charged-particle analyzers, two different programmable high-voltage supplies, twelve 20-bit accumulators and appropriate conditioning and shifting circuitry. Total earth weight is about 6 lbs., and normal power dissipation is 3.0 watts rising to about 6 watts when the lunar-night survival heater is on. Figure 1 shows CPLEE deployed on the lunar surface.

Each physical analyzer contains five C-shaped Bendix Channeltrons with nominal aperture 1 mm each and one helical "funneltron" with nominal aperture 8 mm. These are shown schematically in Figure 2 and an actual analyzer is shown in Figure 3.

A Bendix Channeltron (and the "funneltron") is a hollow glass tube whose inside surface is an emitter of secondary electrons when bombarded by charged particles, ultraviolet light and so on. In CPLEE the aperture of each Channeltron is operated nominally at ground potential (actually at +16 volts) while a voltage of +2800 or +3200 (selected by ground command) is placed on the other i.e. anode end. Thus, if an incident particle enters the aperture and secondary electrons are produced, these are accelerated and hit the walls to generate more secondary electrons and so on, so that a multiplication of order 10^7 is achieved by the time the pulse arrives at the anode.

After conditioning pulses from each Channeltron are accumulated in its own register, for later readout as described below.

As shown in Figure 2, incident particles enter an analyzer through a series of slits and the pass between two deflection plates across which a voltage can be applied. Thus, at a given deflection voltage, the five Channeltrons make a five-point measurement of the energy spectrum of charged particles of a given polarity (say electrons), while simultaneously the funneltron makes a single wide-band measurement of particles with the opposite polarity (say protons). The advantages of simultaneously measuring particles of opposite polarity and also of simultaneous multiple spectral samples are considerable in studies of rapidly-varying particle fluxes.

The CPLEE particle analyzer is quite similar to the device code-named SPECS (O'Brien, et. al., 1967) and in fact the SPECS instrument was the prototype of the CPLEE analyzer.

The capability of SPECS was demonstrated by a series of sounding rocket flights in 1967 and 1968 (Reasoner, et. al., 1968; Westerlund, 1968) and on the Rice/ONR Satellite Aurora 1 (Burch, 1968; Maehlum, 1969). We emphasize that the basic particle analyzer of CPLEE was a flight-proven instrument some 3 years prior to the Apollo 14 mission.

On CPLEE the deflection plate voltage, in the normal mode, is stepped in the sequence shown in Figure 4. As a consequence, the energy passbands shown in Figure 5 are sampled. Although data acquired by the six sensors are not transmitted simultaneously, of course, in practice the six sensors are connected to six accumulators for exactly the same time, viz. 1.2 seconds, and the contents transferred to shift registers for later transmission.

There are two analyzers, A and B, pointing as shown in Figure 6. The same deflection voltage is applied to each analyzer simultaneously, with counts from the 1.2 second accumulation time of Analyzer A being transmitted while counts from B are accumulating. Thus, each voltage is normally on for 2.4 seconds, so that the total cycle time is 19.2 seconds (see Figure 4), when allowance is made for two sample times when the deflection voltage is zero. On one of those two occasions, counts are accumulated as usual, so as to measure "background" or contaminating radiation. On the other occasion a pulse generator of about 300kHz/sec is connected to the accumulators to verify their operation.

The command link with the Apollo Lunar Surface Experiments Package (ALSEP) provides a variety of options on

CPLEE operation. Aside from the usual power commands common to all ALSEP experiments, there are three commands which allow the normal automatic stepping sequence to be modified. The sequence can be stopped and then the deflection plate supply can be manually stepped to any one of the eight possible levels. This is done if one wishes to study a particular phenomena (e.g. low-energy electrons) with higher time resolution (2.4 seconds). A second set of commands allows the Channeltron high voltage supply to be set at either 2800 or 3200 volts, the higher voltage being anticipated for use in the event the Channeltron gains decrease during lunar operations. A third pair of commands allows the normal thermal control mode to be bypassed in the event of failure of the thermostat, offering manual control of the heaters.

CPLEE apertures were covered with a "dust cover" during deployment and LM ascent so as to avoid their contamination particularly by LM-ascent effects (O'Brien et al., 1970a,b). This dust cover was made doubly useful because a Ni^{63} radioactive source was placed on the underside over each aperture. Thus the sensors were proof-calibrated on the moon, and the data compared (see below) with measurements made in the same way with the same system about 14 months previously when the unit was last available for calibration.

B. Calibration

Calibration of the CPLEE's was very extensive and it will be described in detail elsewhere. The major calibration was carried out with an electron gun firing a large, uniform beam of electrons of variable energy, monoenergetic to some 2%.

The instrument was tilted at various angles to the beam under control of an SDS-92 computer, which stored the count rates of each channel at each angle and electron energy, as well as the beam current measured by a Faraday cup. The absolute geometric factors were then computed from the several million measurements accrued.

In addition, the Ni^{63} sources were used as broadband near-isotropic electron sources for standard calibrations.

In practice, the exact passbands were derived, rather than the "rectangular" equivalent passbands of Figure 5. However, these finer details, together with our knowledge of the measured susceptibility to ultraviolet light and to scattered electrons can be shown to be negligible for this preliminary study.

C. Deployment

CPLEE was deployed by astronauts Alan Shepard and Edgar Mitchell at approximately 1800 GMT on February 5, 1971. Leveling to within 2.5° and east-west alignment to within $\pm 2^\circ$ were to be accomplished with a bubble level and a sun compass, respectively. To quote Astronaut Mitchell from the transcript of the scientific debriefing (NASA/MSF, 1971)

"It deployed very nicely. That experiment didn't turn over and that's the one I expected to."

We have since determined by a careful study of the photographs and a comparison of predicted and actual solar ultraviolet response profiles that the experiment is 1.7° off level, tipped to the east and 1° away from perfect east-west alignment, well within the pre-flight specifications.

Furthermore, the photographs (see Figure 1) shows no visible dust accretion on the exterior surfaces. All of these facts attest to the ease of deployment of the CPLEE.

D. Operation of the Experiment

The CPLEE instrument was first commanded on at 036/19/01/03 during EVA #1 for a brief functional test of five minutes duration. All data and housekeeping channels were active, and the instrument began operation in the proper initial modes, i.e. automatic sequencer ON, Channeltron voltage increase OFF, and automatic thermal control.

A complete instrument checkout procedure was initiated at 037/04/00/00 and continued until 037/06/10/00. During this period, data from the dust cover beta sources was accumulated and compared with pre-launch calibrations. A partial comparison is shown in a later section of this report. Also during this period, all command functions of CPLEE were exercised except the forced heater mode and dust cover removal commands. The instrument responded perfectly to all commands. After the checkout procedure, the instrument was commanded to standby to await LM ascent.

Following LM ascent, CPLEE was commanded ON at 037/19/10/00 and the dust cover was successfully removed at 037/19/30/00. The instrument immediately began returning data on charged particle fluxes in the magnetosphere.

The instrument temperatures during the first lunar month were carefully and continuously monitored. It was found that the temperature range was entirely nominal, with the internal electronics temperature ranging from +58°C at lunar noon to

-24°C at lunar night. The total lunar eclipse of February 10, 1971 offered an excellent opportunity to determine various thermal parameters and to test the capability of the instrument to survive extreme thermal shocks. Figure 7 is a plot of the physical analyzer temperature during the eclipse. The maximum thermal shock occurred after umbra exit, with a ΔT rate of 25°C/hour. Also from this figure we can derive a thermal time constant of approximately 1.9 hours. CPLEE suffered absolutely no ill effects from this period of rapid temperature changes.

The command capability of CPLEE was used extensively during the 45-day real-time support period to optimize scientific return from the instrument. Alternate 1-hour periods of manual operation at the -35 volt step and automatic operation have been used to concentrate on rapid temporal variations in low-energy electrons. Similarly, alternate periods of +350 volt manual and automatic operation have been used to focus on rapid changes in magnetopause ions and the solar wind. In fact, the manual operation capability and the attendant 2.4 second sampling interval made possible detection of phenomena which would have been impossible to detect otherwise because of sampling problems and aliasing. Most of the decisions concerning operational modes were based on viewing the real-time data stream, illustrating the desirability and even necessity of the continuous real-time data viewing and command capability during the initial period of ALSEP operation.

As of this writing (March 12, 1971) CPLEE has been operated continuously with all high voltages ON except for one brief period of approximately 15 seconds duration

when it was commanded to standby and then back to ON in order to restore automatic thermal control at the termination of the first lunar night. Absolutely no evidence of high voltage discharge or corona has ever been observed.

IV. Results

We now turn to a detailed discussion of the scientific phenomena observed by CPLEE which were listed in the introduction. These phenomena are in many cases quite distinct, and hence each phenomena complete with data, discussion, and conclusions will be presented in turn.

A. Beta Source Tests

In Table 1 are presented abbreviated results of three separate beta source tests, or data from the CPLEE excited by the Ni^{63} beta sources mounted under the dust cover. (See above.) These three occasions were a) prior to the complete laboratory calibration, b) immediately following the laboratory calibration, and c) after lunar deployment. Note that these tests span a time interval of some 15 months.

The counting rates tabulated are for deflection voltages of -3500 volts for channels 1-5 and +3500 volts for channel 6, or when the channels were sensitive to electrons with energies between 5 kev and 50 kev. We note that the variations in Analyzer A are not more than 20% with 4-6% being typical. In Analyzer B there was a general trend of gain loss between the pre-calibration and post calibration tests in the neighborhood of 20% but there was a partial recovery between the post-calibration test and the post-deployment test. This effect is attributed to the well-known property of temporary Channeltron fatigue due to exposure to high fluxes (e.g. during the calibration) and later recovery. This phenomenon has been documented previously, for example Egidi, et. al. (1969). These beta source tests show that no major changes

occurred in the Channeltron characteristics between calibration and deployment, verified the operation of CPLEE, and we judge the small variations in gain observed to be expected and quite tolerable.

B. Photoelectron Fluxes

One of the most stable and persistent features in the CPLEE data is the presence of low energy electrons whenever the lunar surface in the vicinity of ALSEP is illuminated by the sun. We were able early in the mission to prove these fluxes were of photoelectric origin, by observing the disappearance of these fluxes during the total lunar eclipse of February 10, 1971. In Figures 8 and 9 are shown the counting rates of channel 6 at +35 volts deflection (sensitive to electrons with $50 \text{ ev} < E < 150 \text{ ev}$) of both Analyzers A and B prior to, during, and after the eclipse. The flux is seen to correlate exactly with the presence of illumination, and furthermore it is seen that during the eclipse sporadic burst of electrons presumably of magnetospheric origin occurred with flux levels which are normally undetectable due to the masking effect of the photoelectrons.

The energy spectrum of these photoelectrons, obtained from channels 1-5 at -35 volts at a period just prior to eclipse onset is shown in Figure 10 for both Analyzers. As one would expect, the spectrum is quite steep, as we are observing essentially a high energy, possibly non-thermal, tail of an electron distribution with an average energy on the order of 2 ev. (Walbridge, 1970). In fact, the high-energy tail which we measure is almost certainly non-thermal, for the spectrum between 40 and 100 ev can be represented by an equation of the form: $j(E) = j_0 \exp \left[\frac{-(E-40)}{14.7} \right]$. Clearly this does not agree with a simple Maxwellian distribution at low energies with $kT \sim 2 \text{ ev}$. There are two possible explanations for this discrepancy, one being that

some process is acting to accelerate part of the photoelectron gas, the other being that the CPLEE itself is at a positive potential with respect to the surrounding lunar surface average potential. This is entirely possible in view of the fact that CPLEE is well insulated from the lunar surface by fiberglass legs and that the photoemission properties of CPLEE and of the lunar surface are almost certainly quite different. We hope to be able to resolve this question with detailed studies of these photoelectron fluxes especially during periods of terminator crossings and the eclipse.

It should also be noted that although in one sense the photoelectron fluxes are a contaminant obscuring weak fluxes of magnetospheric origin (see Figure 8), they are valuable not only because they furnish information of solar radiation - lunar surface interactions, but also because they furnish a stable "calibration source" for monitoring long-term changes in Channeltron operating characteristics. To put it another way, the photoelectrons offer a continuing "beta-source" test for monitoring the performance of the instrument.

C. Lunar Module Impact Event

The Apollo 14 Lunar Module Antares ascent stage impacted the lunar surface on February 7, 1971 at 00 hours, 45 minutes, 24 seconds G.M.T. at lunar LOC-2 coordinates 3.42° south and 19.67° west, or 66 km. west of the CPLEE. The terminal mass and velocity were 2303 kilograms and 1.68 km/sec respectively, resulting in an impact energy of 3.25×10^{11} joules. (Latham, private communication). The LM contained approximately 180 kilograms of volatile fuels, primarily dimethyl hydrazine ($\text{CH}_3\text{NHNHCH}_3$) and nitrogen tetroxide (N_2O_4). For the purpose of reference and orientation, Figure 11 is a lunar map showing the location of the impact point relative to the Apollo 12 and Apollo 14 ALSEPs.

In Figure 12 we show the counting rates of channel 6 of Analyzer A, measuring ions with energies of 50 ev to 150 ev per unit charge and channel 3 of the same analyzer, measuring negative particles with energies of 61 to 68 ev for the period 00/44/53 G.M.T. to 00/48/55 G.M.T. on February 7, 1971. The Antares impact, as seen from the figure and Figure 11, occurred at 00/45/24 G.M.T. at a point 66 km almost due West of CPLEE.

As can be seen from Figure 12, the counting rates prior to and during Antares impact were reasonably constant, and by all indications were due to the ambient population of low energy electrons and ions which are present whenever the lunar surface in the vicinity of CPLEE is illuminated. (This conclusion is supported by the observation that these ambient fluxes disappeared entirely during the total lunar eclipse which occurred a few days later on February 10, 1971, as shown in Figures 8 and 9). The counting rates increased by a factor of about four some 40 seconds after impact and then reverted to ambient levels for a

few seconds. However, at $T + 48$ seconds the ion and electron counting rates increased very rapidly by a factor of up to forty as the plasma cloud enveloped CPLEE. A second plasma cloud passed CPLEE a few seconds later, as shown by the second large peak. On the assumption that the plasma clouds travelled essentially in a linear path between the impact point and CPLEE, we calculate an average velocity of 1.0 km/sec and horizontal dimensions of 14.4 km and 7.2 km for the first and second clouds, respectively.

Figure 13 shows the same data for Analyzer B oriented 60° from vertical toward lunar West (i.e. toward the impact point). From comparison of Figures 12 and 13 one can note that the flux enhancements were essentially simultaneous in the two directions, but the ion flux measured by Analyzer A was 5 times higher than the flux measured in Analyzer B. On the other hand, the negative particle flux measured by Analyzer A was only $1/3$ as great as the negative particle flux measured by Analyzer B.

The detailed characteristics of the plasma clouds are shown in Figure 14, a plot on an expanded time scale of the negative particle fluxes in five energy ranges and the ion flux in a single energy range measured by Analyzer A. The plot shows clearly that the negative particle enhancement was confined to energies less than 100 ev, as the 200 ev flux was essentially constant throughout the event. Furthermore, it is seen that the spectrum of negative particles during the enhancement is quite different from the background electron spectrum. This point is illustrated further in Figure 15, showing the negative particle spectra for the times 038/00/42/38 (prior to the Antares impact) and 038/00/46/32 (at the peak of the first plasma cloud).

It might well be questioned whether the flux enhancements at $T + 48$ and $T + 67$ seconds were actually initiated by the Antares impact. Indeed, in the time period of approximately 2 days following the impact event, several rapid enhancements in the low-energy electron fluxes by up to a factor of 50 were observed. However, these other enhancements were not correlated with ion flux increases, and in fact the event referred to here is the only such example of such perfectly correlated ion and negative particle enhancements seen to date. In addition, careful monitoring prior to the impact revealed that the fluxes were relatively stable, constant to within a factor of 2 over time periods of a few minutes. This lends credence to the belief that we have here a valid case of cause and effect.

Further confidence in our interpretation that the flux enhancements were artificially impact-produced rather than of natural origin is gained by noting that although no such plasma clouds have previously been detected resulting from impact events, Freeman, et.al. (1971) have reported detection of ion clouds with the Apollo 12 SIDE instrument apparently resulting from the Apollo 13 and 14 Saturn IV-B stage impacts, the powered ascent and descent phases of the Antares, and from this, the Antares impact. (Freeman, private communication)

We now turn to a discussion of some of the detailed parameters calculated from the flux enhancements. We have previously noted an average cloud velocity of 1 km/sec, and it is of interest to compare this with particle velocities in the cloud. Some assumptions must of course be made as to the ion species present, and considering that the most likely source of ions was the LM fuels we estimate an average ion mass of 25. If we assume the negative particles detected were electrons and the positive

particles had an average mass of 25, this yields velocities ($E = 50$ ev) of 4000 km/sec and 20 km/sec respectively. The charged particle energy density based upon the ions actually measured is calculated to be 5.6×10^{-10} ergs/cm³, assuming the ions were protons, and 28.0×10^{-10} ergs/cm³ assuming an average ion mass of 25. We emphasize that these are lower limits, as we measured ions in only a single energy range, and hesitate to assume an overall ion energy spectrum in order to make a more exact calculation. The magnetic field energy density at the lunar surface, based on Apollo 12 Lunar Surface Magnetometer measurements (Dyal, et al., 1970) of a steady 35 γ field is 50×10^{-10} ergs/cm³, and hence it appears that the particle energy density is at least comparable to and possibly dominant over the magnetic field energy density. We also point out that the solar wind energy density is 80×10^{-10} ergs/cm³.

We therefore conclude that the Antares impact resulted in the production of two annular plasma clouds which contained negative particles and ions with energies up to 100 ev and travelled across the lunar surface with a velocity on the order of 1 km/sec. We do not speculate as to the mechanisms responsible for production of these clouds, but only note that the simultaneous arrival of both positive and negative charge species is impossible to reconcile with a simple model of photo-dissociation and ionization and subsequent acceleration by a static electric field.

The fact that the electron and ionic components were detected simultaneously offers a unique problem, for if one assumes that the particles were energized at the instant of impact, one must find a mechanism that is able to hold the

cloud together, in view of the fact that measured ion velocities exceed the cloud velocity by an order of magnitude. This fact in itself argues against ambipolar diffusion. Processes such as charge exchange, scattering, and wave-particle interactions can also be rejected by appealing to considerations based on the size of the clouds (~ 10 km). The only remaining possibility is magnetic confinement, or a process whereby the local magnetic field confines the particles in circular orbits. There are however two criticisms of magnetic confinement. The first is, that in order for the mechanism to operate, the energy density in the magnetic field must dominate the energy density of the particles. We have shown above, however, that this is quite probably not the case. The second is that the cyclotron radii of the particles must be no greater than the dimension of the plasma cloud. The cyclotron radius of a 50 ev, mass 25 ion in a 35 gauss magnetic field is 150 km, or a factor of ~ 10 larger than the inferred cloud dimensions.

It thus appears that a simple model of the particles being energized at the instant of impact is untenable not in itself, but because a mechanism to contain the plasma after energization is not readily apparent, and in fact may not exist. The alternate conclusion is then that the impact produced expanding gas clouds, and the particles in these gas clouds were then ionized by any one of several means (e.g. photoionization) and subsequently accelerated by a continuously active acceleration mechanism. We note that the solar magnetospheric coordinates of CPLEE at the time of impact were $Y_{SM} = 34 R_E$ and $Z_{SM} = 21 R_E$, and the solar elevation angle was 30° . Hence it is highly likely that the solar wind had direct access to the lunar surface at this time. Noting the energy densities of the solar wind and the

plasma cloud particles (see above), it is seen that the solar wind is energetically capable of being the energy source, but whether or not any such mechanism can work is unknown at this time, although calculations by Lehnert (1970) have indicated that the solar wind can interact with a neutral gas through means other than simple particle-particle collisions.

In summary, it would appear that the impact event data indicates a situation where the gas cloud, solar wind, and local magnetic field are all interacting, offering a unique and fascinating problem in plasma physics.

D. Low Energy Electron Fluctuations

In addition to the stable low energy photoelectron population which CPLEE observes whenever the lunar surface in the vicinity is illuminated (see above), for some 5-10% of the lunar day CPLEE observes rapidly varying fluxes of low energy electrons of magnetospheric origin, with intensities large enough to be detected above the photoelectron background. Such an example of these fluxes is shown in Figure 16, wherein the counting rates of channel 3 (65 ev electrons) and channel 5 (200 ev electrons) are plotted for a brief time segment. At this time, February 7, 1971 at approximately 2120 G.M.T., the solar magnetospheric coordinates of CPLEE were $Y_{SM} = 24 R_E$ and $Z_{SM} = 14 R_E$, locating the instrument within the tail near the boundary. The instrument was in manual mode at this time, and hence the individual measurements are 2.4 seconds apart. The flux enhancements are seen to range up to a factor of 10 above the background level on time scales on the order of a few seconds. At first glance it appears that the enhancements in the two energy ranges are well correlated, but a closer examination of the figure reveals temporal dispersions in the enhancements. To illustrate this point more clearly, the data for the period 21/20/07 G.M.T. to 21/20/41 G.M.T. have been plotted in a rather unique manner in Figure 17, in that a log - log plot of the counting rates in the two energy channels was made with the higher energy channel on the vertical axis and the lower energy channel on the horizontal axis. Each pair of points from the two channels is represented by a single point, and a vector is drawn between successive points in the direction of increasing time. On this sort of plot, if the enhancements are perfectly correlated, then all vectors will lie along a constant slope whose magnitude is a function of the relative enhancements. A burst where the higher

energy electrons lead the lower energy electrons will result in an open figure with the vectors rotating clockwise, and likewise if the higher energy electrons lag the lower energy electrons the vectors will rotate counterclockwise. An examination of this figure shows that in general for the longest vectors the constant slope rule is followed, but that on smaller scales (for example points 1 to 5 and 9 to 12) there are considerable deviations from the constant slope rule, and for these events the vectors rotate clockwise indicating that the higher energy electrons lead the lower energy electrons. Although plots such as these are indicative in nature, they do show the general character of the enhancements, and suggest that low energy electrons are being accelerated or modulated by processes relatively near the moon. A rough estimate of the distance can be obtained by considering the velocity difference at the two energies and the dispersion times in the enhancements (0 seconds to ~ 2 seconds), resulting in a maximum distance of some 20,000 kilometers, or $3 R_E$. An extensive cross correlation analysis will be necessary to refine these calculations, but these preliminary studies do indicate the presence of local (w.r.t. the moon) processes capable of modulating or accelerating low energy electron fluxes.

E. Medium Energy Electron Event

On March 10, 1971 at approximately 1830 G.M.T. distinct enhancements in medium energy (~ 1 kev) electron fluxes were observed in both Analyzers A and B. The enhancements ranged up to a factor of 10 above background and had durations lasting from a few minutes up to 2 hours, and the entire event lasted approximately 4 hours. In order to examine the gross temporal features of these enhancements, we have plotted in Figure 18 the counting rate of channel 6 at +350 volts (500-1500 ev electrons) for the period 1830 to 2300 G.M.T. The data gaps at 1930 and 2130 were due to the fact that CPLEE was in manual mode at -35 volts at these times, and the data gap at 2100 was due to a temporary loss of the data decommutation computer at M.S.C.

It is seen from the figure that the event is characterized by erratic , relatively short duration flux enhancements between 1830 and 2100, a period of stable high fluxes between 2110 and 2200, and a return to erratic enhancements between 2200 and 2300. Auxiliary data which should be mentioned was kindly supplied by Mr. Bob Doeker of E.S.S.A. The K_p index was .34 or less on March 10 and there were no enhancements in the solar x-ray flux. Thus it appears that this event is characteristic of the quiet time magnetosphere, and the electrons are truly magnetospheric in origin.

We are unable in this case, based on the particle measurements alone, to resolve the question of whether the enhancements are of spatial or temporal nature, that is whether we are seeing the effects of CPLEE moving in and out of stable spatial region (s) of flux enhancements or whether we are seeing a large scale temporal event. The cyclotron radius of a 1 kev electron

in a 10γ field, typical of the magnetic tail at lunar distances (Ness, et.al., 1967), is 10.6 kilometers, and the moon moves a distance of ~ 20 kilometers between data samples.

The path of CPLEE in the solar magnetospheric Y-Z plane is shown in Figure 19. Of particular interest is the fact that the event was seen only during the period when Z_{SM} was near the maximum positive excursion of $6 R_E$. This is highly suggestive, though certainly not proof conclusive, that CPLEE was sampling a stable spatial structure located at $Z_{SM} = + 6 R_E$ and $Y_{SM} = 11-13 R_E$.

The electron energy spectrum, averaged over the time period 2145 to 2200 G.M.T., the period of the most stable fluxes (see Figure 18) is shown in Figure 20. The photoelectron continuum is the dominant contribution between 40 and 100 ev, but there is a suggestion of a peak in the spectrum of these magnetospheric electrons at 600 ev. Also shown is an upper limit to the background equivalent flux from all other sources at 500 ev, showing the order of magnitude enhancement seen in the event. The integrated flux for electrons with energies between 500 and 2000 ev is 4.5×10^6 electrons/cm² - sec - ster.

The energy spectrum and total flux of electrons and the temporal history of the event all suggestive that these data represent an observation of the neutral sheet. The difficulty with this interpretation lies in the fact that at this time CPLEE was some $6 R_E$ away from the theoretical location of the neutral sheet, the Y_{SM} axis. (See Figure 19). There are strong indications however that the solar-magnetospheric coordinate system is unable to locate the neutral sheet with an error less than $\sim 10 R_E$ at lunar distances. The neutral sheet observations of Speiser and Ness (1967) with a magnetometer

on-board the IMP 1 satellite locate the neutral sheet at various times during the period March 22 to May 26, 1964 in the range $-2R_E < Z_{SM} < 5R_E$. Hence, it is quite plausible that the neutral sheet could have been located at $Z_{SM} = 6R_E$ at the time of the CPLEE observation. Further measurements during forthcoming magnetotail passes by CPLEE are needed to effect a definite resolution of this question.

F. Electron Spectra Similar to Auroral Spectra

On several occasions when CPLEE was in the magnetospheric tail, short-duration electron enhancements in all ranges of the instrument were observed. These enhancements typically had durations of a few minutes. The energy spectrum of one such enhancement on February 7, 1971 at 2316 G.M.T. is shown in Figure 21. As in all electron spectra observed when the lunar surface is illuminated, the spectrum between 40 ev and 100 ev is dominated by the photoelectron continuum. However in the higher energy ranges is seen a double peak structure, with a low energy peak in the range 300-500 ev and a high energy peak at 5 kev. It is interesting to compare this spectra with spectra observed above a terrestrial aurora. Figure 22, from Westerlund (1968), shows a set of spectra observed above an aurora, measured with a SPECS detector on board a Javelin sounding rocket. It should be recalled that the basic particle detectors of both the SPECS and CPLEE are very similar. The photoelectron continuum is of course absent from these auroral spectra, but aside from that a remarkable similarity between the electron fluxes observed by CPLEE and the auroral electrons is readily apparent. Note particularly the double peak structure in both spectra, the low energy peaks in the 100-500 ev range, and the high energy peaks at 5-6 kev. The flux levels in the auroral spectrum are within a factor of 5 of the flux levels measured by CPLEE (see Figure 21). Furthermore, while particles measured above auroras tend to be more or less isotropic about the field lines, the magnetic tail particles observed by CPLEE were strongly peaked along the field lines. This

was deduced by noting that there were no flux enhancements in Analyzer B, and that the angles between the magnetic field and the directions of Analyzers A and B were approximately 20° and 80° , respectively.

One would of course expect that particles energized near the earth and subsequently traveling back into the tail would be sharply peaked along field lines at lunar distances according to the 1st invariant $\sin^2 \alpha/B = \text{constant}$.

It would then appear that the process which produces energetic particles above terrestrial auroras may well result in the appearance of similar particles in the magnetospheric tail. A definite resolution of this question awaits further study of the data and correlation between CPLEE data and earth-based measurements of auroral activity. However, this preliminary indication of auroral particles at large distances from the earth in the magnetotail implies that some auroral zone magnetic field lines are linked with field lines stretching far into the tail, and hence gives information on the general topology of the magnetosphere.

G. Rapid Temporal Solar Wind Variations

When the moon crosses from the tail regions into interplanetary space on the dawn side of the magnetosphere, CPLEE Analyzer B is pointed toward the sun and hence is able to detect solar wind fluxes striking the moon. Some of the detailed characteristics of solar wind at the lunar surface have been reported by Snyder et. al. (1970), and we state here that the CPLEE measurements are in general agreement with the measurements of average solar wind parameters by the Solar Wind Spectrometer on Apollo 12. We have however used the unique rapid-sampling capability of CPLEE to study temporal variations in the solar wind. We compare the sampling interval of CPLEE (2.4 seconds) with those of other experiments designed to measure solar wind fluxes, notably the Vela 3A and 3B detectors with sampling intervals of 256 seconds (Gosling, et. al., 1968) and the Solar Wind Spectrometer sampling interval of 28.1 seconds (Snyder, et. al., 1970).

In Figure 23 we show an example of such rapid solar wind variations. At this time, February 16, 1971 at 2045 G.M.T. the solar magnetospheric coordinates of CPLEE were $Y_{SM} = -67 R_E$ and $Z_{SM} = -32 R_E$, placing the instrument some 20 - 30 R_E away from the magnetospheric tail boundary. The angle between the center of the detector field of view and the CPLEE-sun line was 2° . The CPLEE data showed the counting rate was concentrated in channel 5 at +350 volts deflection, or the channel sensitive to ions with energies between 1.5 and 3.0 kev, exactly what would be expected if the instrument were viewing the direct solar wind. The ratio of the counting rates of this channel in Analyzer B

to the corresponding channel in Analyzer A was on the order of 1000:1, indicating the extreme directionality of the flux.

The figure shows variations in the solar wind flux of up to a factor of 10 on time scales as short as 5 seconds. We assert that these variations are indeed temporal in nature, by simply comparing the cyclotron radius of a 1.5 kev proton in the 5 γ interplanetary field (1000 km) with the linear velocity of the moon (1 km/sec). If the variations were spatial in origin, this would require variations in the flux of a factor of 10 over distances as short as 1/200 of a cyclotron radius, a situation we deem highly unlikely.

We point out that we have by no means selected an isolated feature of the data, and assert that these rapid temporal variations are a persistent feature of the solar wind flux. Lacking a detailed analysis of the frequency spectra of these variations, we can only speculate at this time as to their origin. We note, however, that the observed frequency of variations ($\sim .2$ c.p.s.) is similar to the expected observed frequency of magnetosonic waves in the solar wind whose wavelength is on the order of an ion cyclotron radius, as seen by a stationary observer ($\sim .5$ c.p.s.). This is suggestive that the variations we see are due to magnetosonic waves modulating the particle fluxes, and these waves may be generated at the shock surface between the solar wind and the magnetospheric.

V. Summary

During the first month of operation CPLEE has detected particle fluxes at the lunar surface resulting from a wide range of lunar surface, magnetospheric, and interplanetary phenomena. Preliminary data analysis has revealed that presence of a lunar photoelectron layer, an indication of modulation or acceleration of low energy electrons in the vicinity of the moon, penetration of auroral particles to lunar distances in the tail, detection of electron fluxes in the tail quite possible associated with the neutral sheet, strong modulations of solar wind fluxes, and the appearance of ions and electrons with energies up to 100 ev associated with the Lunar Module impact. It should be emphasized that many of these discoveries were possible only because of the rapid sampling capability of CPLEE and its ability to measure particles of both charge signs over a wide energy and dynamic range, coupled with the real time data display and command capability of the ALSEP system.

These preliminary findings have all resulted from analysis of "quick look" hard copy data. Other phenomena are apparent in the data, but their adequate characterization and description must await detailed computer analysis of the 200 measurements per minute being returned by CPLEE.

Acknowledgements

A very large number of people contributed to the success of CPLEE, both directly and indirectly through development of SPECS and of the calibration equipment. Current and former Rice University personnel who made major contributions are Wayne Smith (program manager), John Musslewhite (program manager until early 1969), James Ballentyne (quality assurance), John McGarity, David Nystrom, William Porter, Foster Abney, James Burch, and Tad Winiecki.

Bendix personnel who played principal roles were Joe Clayton, Park Curry, Al Robinson, Charles Hocking, William Stanley, George Burton, Lou Paine, Lowell Ferguson, John Ioannau, Jack Dye, Mark Brooks, Charles Flint, and Jerome Pfeiffer.

Numerous N.A.S.A. personnel played important roles in many phases of the program. Amongst them must be included Dick Moke, Jack Small, Don Wiseman, Ausley Carraway, J. B. Thomas, and W. K. Stephenson of M.S.C. as well as Dr. J. Naugle and Dr. A. Opp and Ed Davin of N.A.S.A. Headquarters and A. Spinak of Wallops Station.

Finally, we would like to thank Astronauts Alan Shepard, Edgar Mitchell and Stuart Roosa for getting CPLEE to the moon.

This work was supported by National Aeronautics and Space Administration contract NAS9-5884.

References

- Apollo 14 Photographic and Scientific Debriefing, NASA Publication MSC-04033, 1971.
- Burch, James L. "Low-Energy Electron Fluxes at Latitudes Above the Auroral Zone", Jour. Geophys. Res., 73, 3585, 1968.
- Dyal, P., C. W. Parkin, and C. P. Sonnet "Lunar Surface Magnetometer Experiment, Apollo 12 Preliminary Science Report", NASA Publication SP-235, 1970.
- Egidi, A., R. Marconero, G. Pizzella, and F. Sperli "Channeltron Fatigue and Efficiency For Portons and Electrons", Rev. Sci. Instr., 40, 88, 1969.
- Freeman, J. W., Jr., H. K. Hills, and M. A. Fenner "Some Results From the Apollo 12 Suprathermal Ion Detector", Preprint, 1971.
- Gosling, J. T., J. R. Ashbridge, S. J. Bame, A. J. Hundhausen, and I. B. Strong "Satellite Observations of Interplanetary Shock Waves", Jour. Geophys. Res., 73, 43, 1968.
- Lehnert, B. "Minimum Temperature and Power Effect of Cosmical Plasmas Interacting with Neutral Gas", Royal Institute of Technology, Division of Plasma Physics, Stockholm Report 70-11, 1970.
- Lyon, E. F., H. S. Bridge, and J. H. Binsack "Explorer 35 Plasma Measurements in the Vicinity of the Moon", J. Geophys. Res., 72, 6113, 1967.
- Maehlum, Bernt N. "On the High-Latitude, Universal Time Controlled F-layer", Jour. Atm. Terr. Phys., 31, 531, 1969.
- Ness, N. F., K. W. Behannon, C. S. Searce, and S. C. Cantarano "Early Results from the Magnetic Field Experiment on Lunar Explorer 35", Jour. Geophys. Res., 72, 5709, 1967.
- O'Brien, B. J. "Interrelations of Energetic Charged Particles in the Magnetosphere", Solar Terrestrial Physics, ed. Newman and King, Chapter IV, Academic Press, London, 1967.

- O'Brien, B. J., F. Abney, J. Burch, R. Harrison, R. LaQuey, and T. Winiecki "SPECS, A Versatile Space-Qualified Detector of Charged Particles", Rev. Sci. Instr., 38, 1058, 1967.
- O'Brien, B. J., S. Freden, and J. Bates "Degradation of Apollo 11 Deployed Instruments because of LM Ascent Effects", Jour. App. Phys., 41, 4538, 1970a.
- O'Brien, B. J., S. Freden, and J. Bates "Dust Detector Experiment, Apollo 12 Preliminary Science Report", NASA Publication SP-235, 1970b.
- Reasoner, D. L., R. H. Eather, and B. J. O'Brien "Detection of Alpha Particles in Auroral Phenomena", Jour. Geophys. Res., 73, 4185, 1968.
- Snyder, Conway W., Douglas R. Clay, and Marcia Neugebauer "The Solar Wind Composition Experiment, Apollo 12 Preliminary Science Report", NASA Publication SP-235, 1970.
- Speiser, T. W. and N. F. Ness "The Neutral Sheet in The Geomagnetic Tail: Its Motion, Equivalent Currents, and Field Line Connection through It.", Jour. Geophys. Res., 72, 131, 1967.
- Walbridge, Edward "The Lunar Photoelectron Layer 1. The Steady State", Preprint, 1970.
- Westerlund, L. H. "Rocket-Borne Observations of the Auroral Electron Energy Spectra and Their Pitch-Angle Distribution", PhD Thesis, Rice University, 1968.

CPLEE BETA SOURCE TESTS

ANALYZER A

	CH 1	CH 2	CH 3	CH 4	CH 5	CH 6
Pre - Cal. Oct. 24, 1969	8.7	22.2	38.8	80.7	165.7	1280.5
Post - Cal. Jan. 20, 1970	8.2	18.9	38.5	86.6	205.7	1323.0
Post - Deploy Feb. 6 - 1971	10.68	20.5	39.6	82.4	195.9	1259.0

ANALYZER B

	CH 1	CH 2	CH 3	CH 4	CH 5	CH 6
Pre - Cal. Oct. 24, 1969	5.8	12.7	19.8	43.6	113.1	777.7
Post - Cal. Jan. 20, 1970	4.5	9.1	14.6	34.8	96.6	577.9
Post - Deploy Feb. 6, 1971	7.68	12.0	17.8	35.4	90.0	763.8

TABLE 1

Figure Captions

1. Photographs by Astronaut Shepard of the CPLEE instrument deployed on the lunar surface. Note particularly the absence of dust contamination and the east-west alignment.
2. Schematic sketch of the CPLEE physical particle analyzer, showing the deflection plates and Channeltron stack.
3. Photograph of the CPLEE physical particle analyzer.
4. Deflection voltage stepping sequence of CPLEE in the automatic mode. At the +0 step the background level is measured and at the -0 step a test oscillator is injected into the accumulators.
5. The rectangular equivalent energy passbands of CPLEE.
6. A sketch of the CPLEE instrument, showing the fields of view and the look directions of the physical analyzers.
7. Temperature profile of CPLEE during the total lunar eclipse of February 10, 1971.
8. The counting rate of channel 6, Analyzer A at -35 volts, measuring electrons with energies between 50 and 150 ev for the time period including the lunar eclipse.
9. The counting rate of channel 6, Analyzer B at -35 volts, measuring electrons with energies between 50 and 150 ev for the time period including the lunar eclipse.
10. The energy spectrum of photoelectrons with energies between 40 and 200 ev. The sketch on the figure shows the geometry of CPLEE relative to the lunar surface and to the direction of solar radiation.

11. A lunar map showing the locations of the CPLEE and of the Apollo 14 LM ascent stage impact point.
12. The counting rates of channel 3 and channel 6 of Analyzer A at -35 volts, measuring 65 ev negative particles and 70 ev ions respectively, showing the particle fluxes resulting from the LM impact.
13. Same as Figure 12, except showing data from Analyzer B.
14. An expanded view of the data of Figure 12, showing details of the two prominent peaks. In this figure are shown fluxes computed from 5 negative particle energy ranges and a single ion energy range.
15. Electron spectra measured by Analyzer A for two periods. The first is a few minutes prior to impact and the second is the time at the height of the first large peak in Figure 12.
16. An example of rapid variations in magnetospheric low energy electron fluxes. The plot shows data from channel 3 and 5 of Analyzer A at -35 volts, measuring 65 ev and 200 ev electrons, respectively.
17. A detailed study of a portion of the data of Figure 16. The counting rate of channel 5 (65 ev electrons) is plotted vs. the counting rate of channel 3 (200 ev electrons) on a log-log scale. Perfect temporal simultaneity would result in all vectors lying parallel to a line of constant slope. Note the marked deviations from this rule.
18. The medium energy (~ 1 kev) electron event of March 10, 1971. The counting rate of channel 6, Analyzer A at +350 volts is shown, indicating the gross features of the event. For a complete discussion see text.
19. The track of CPLEE in the $Y_{SM} - Z_{SM}$ plane for the period March 10 - March 12, 1971 including the period of the electron event shown in Figure 18.

20. The electron energy spectrum measured by Analyzer A between 40 and 2000 ev for the period 21:45 to 22:00 G.M.T. on March 10, 1971, the period of high, stable flux shown in Figure 18.
21. The electron energy spectrum of a typical "auroral electron" event measured by CPLEE in the magnetospheric tail. Of particular note is the double peak structure, with a low energy peak at 300-500 ev and a higher energy peak at 5-6 kev.
22. Electron spectra measured above a terrestrial aurora by a device similar to CPLEE on a sounding rocket probe, from Westerlund (1968). Note the striking similarities between these spectra and the CPLEE magnetospheric tail electron spectrum shown in Figure 21.
23. An example of rapid temporal variations in solar wind fluxes. Data from channel 5 of Analyzer B at +350 volts, sensitive to ions with energies between 1.5 and 3 kev are plotted with a time resolution of 2.4 seconds.

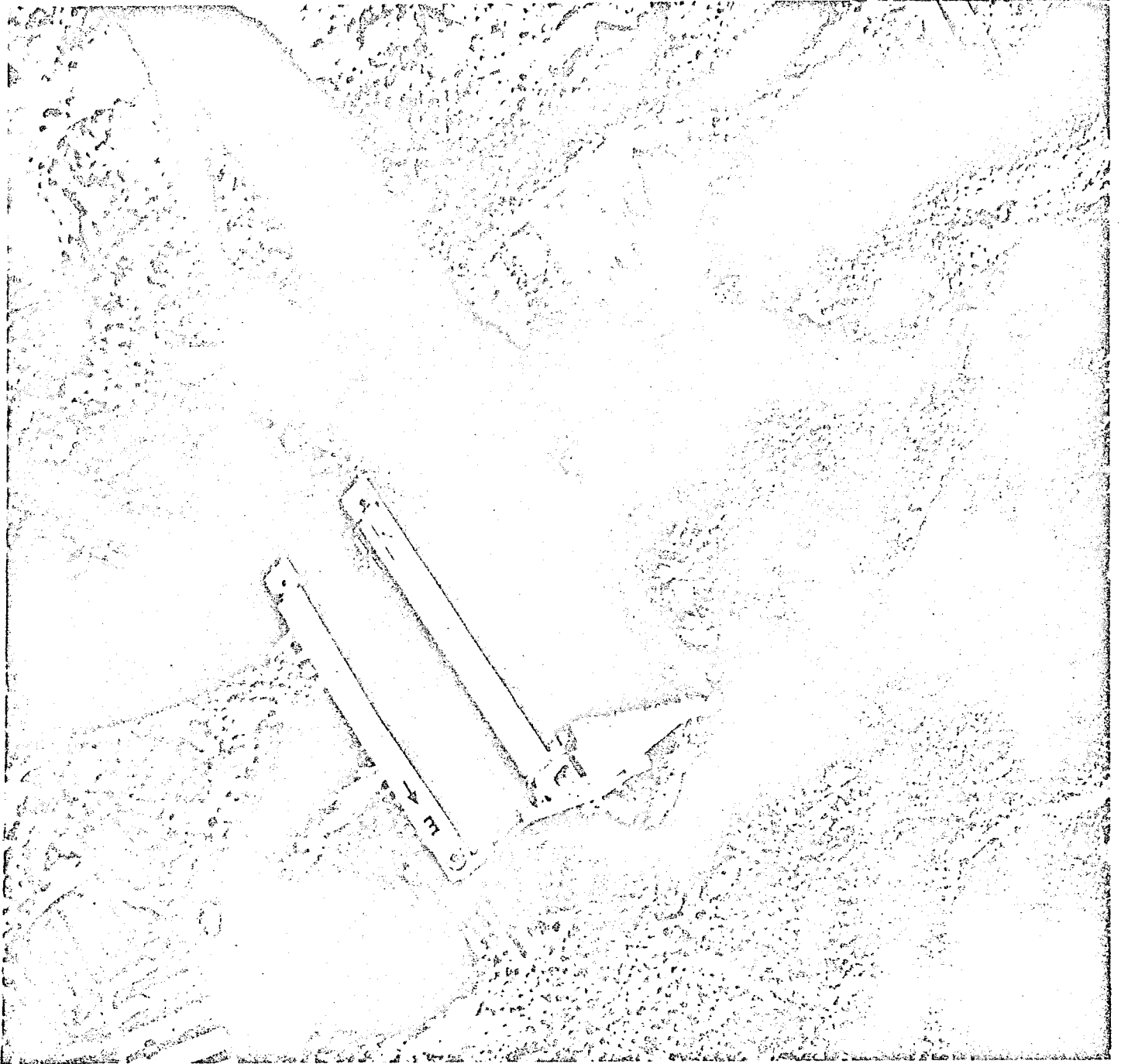


FIGURE 1

CPL-EE PHYSICAL ANALYZER

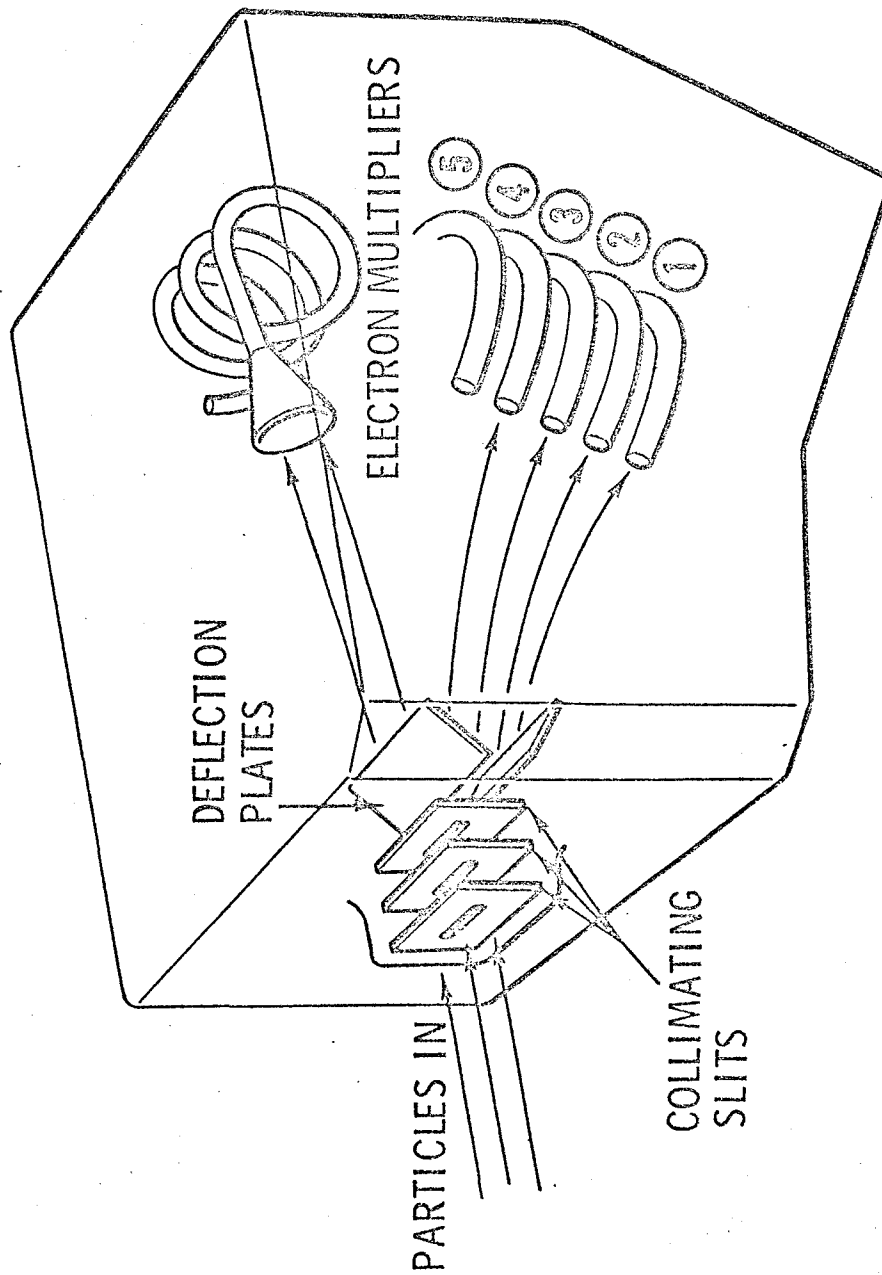


FIGURE 2

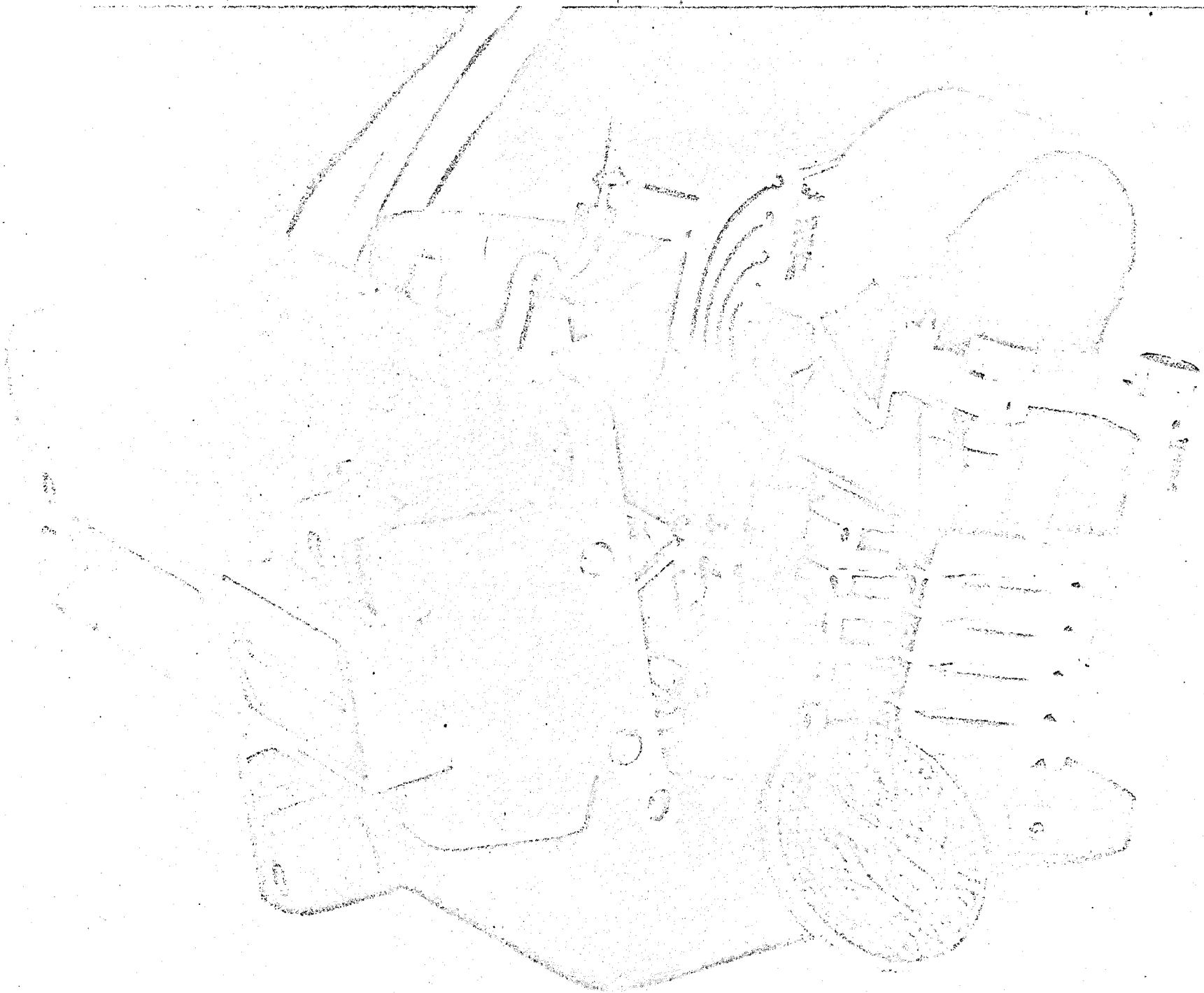


FIGURE 3

CPLLEE TIMING SEQUENCE

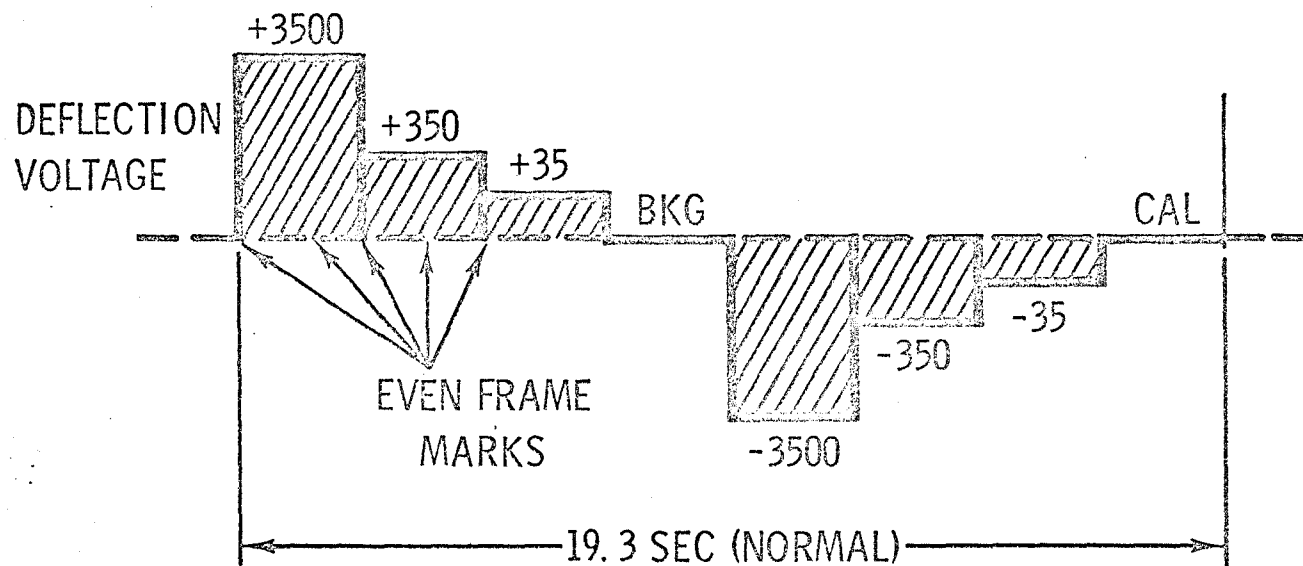
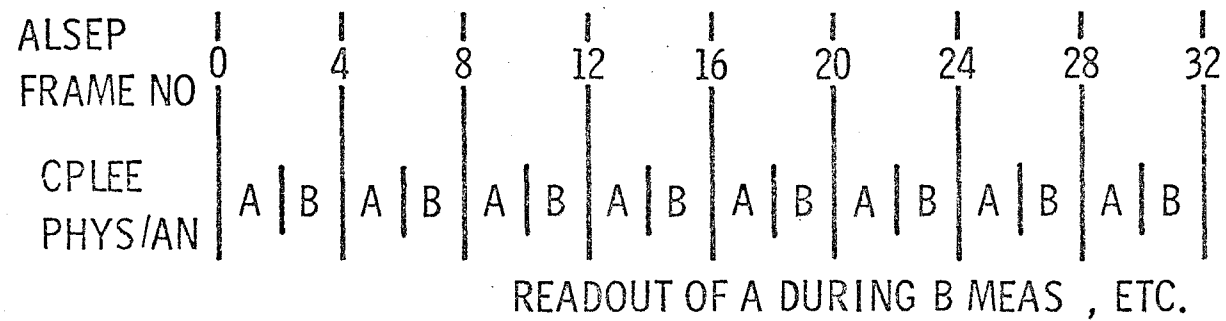


FIGURE 4

CPLEE ENERGY PASSBANDS

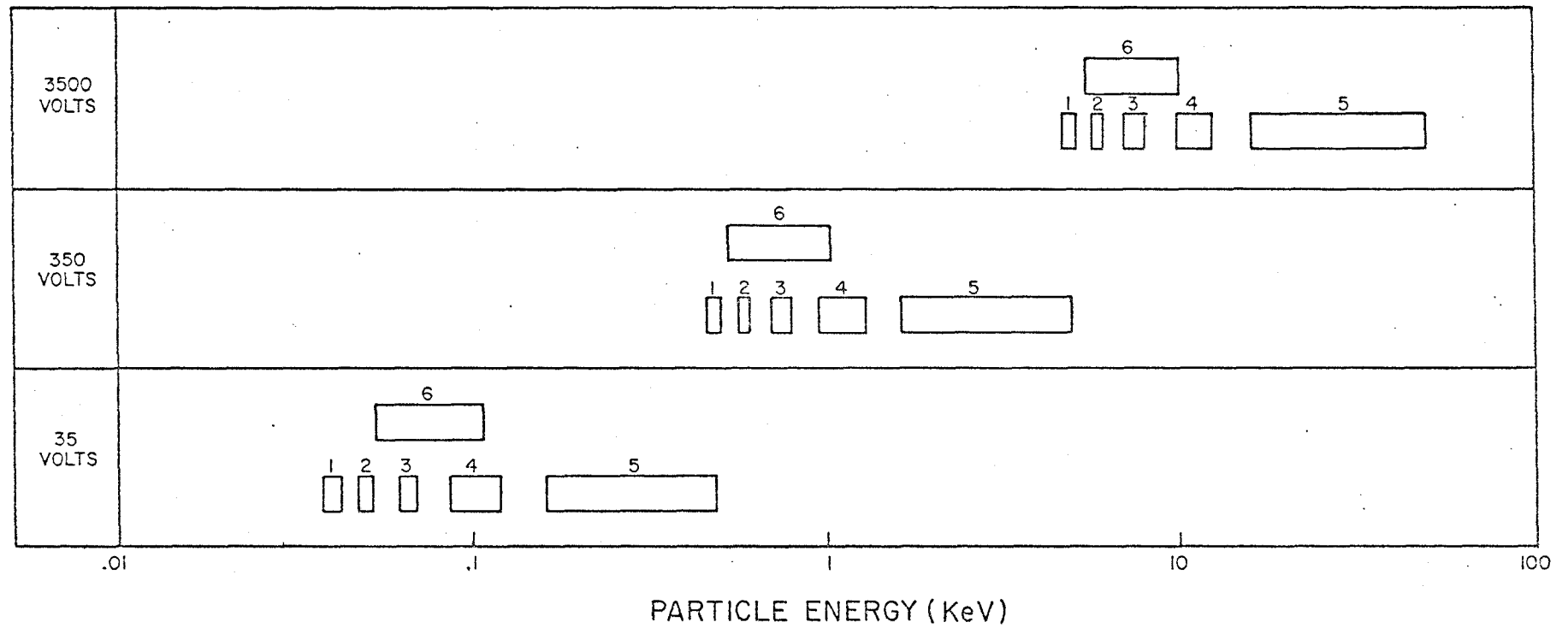


FIGURE 5

CHARGED-PARTICLE LUNAR ENVIRONMENT EXPERIMENT SUBSYSTEM

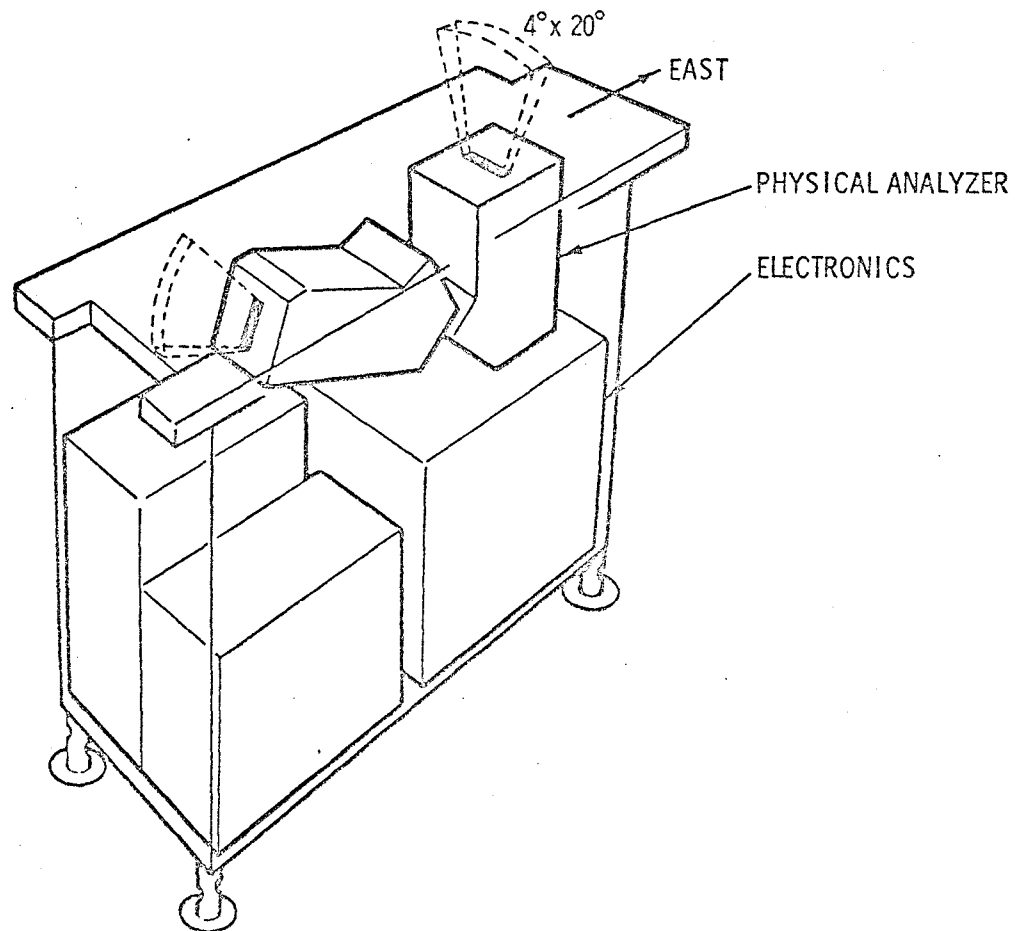


FIGURE 6

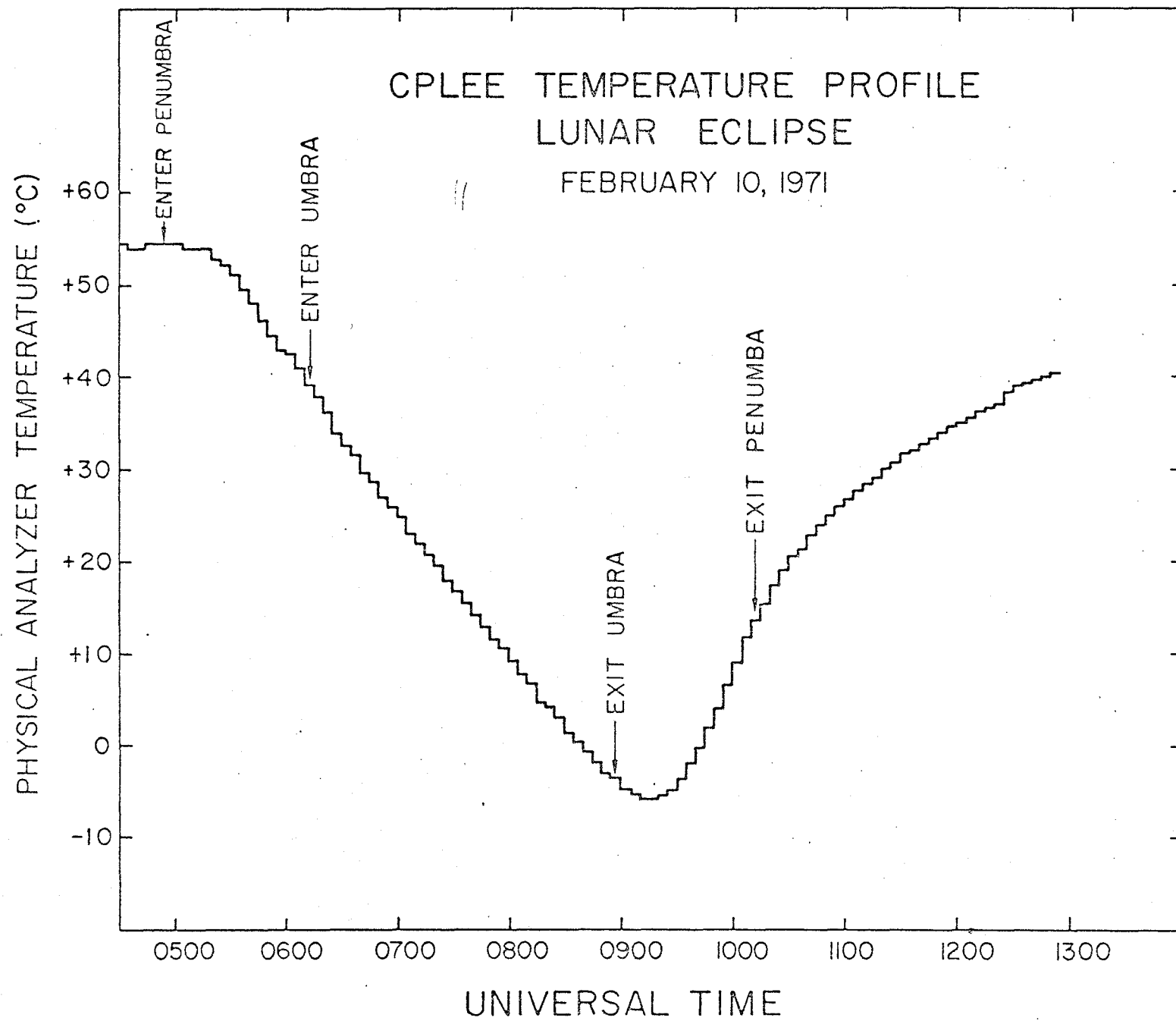


FIGURE 7

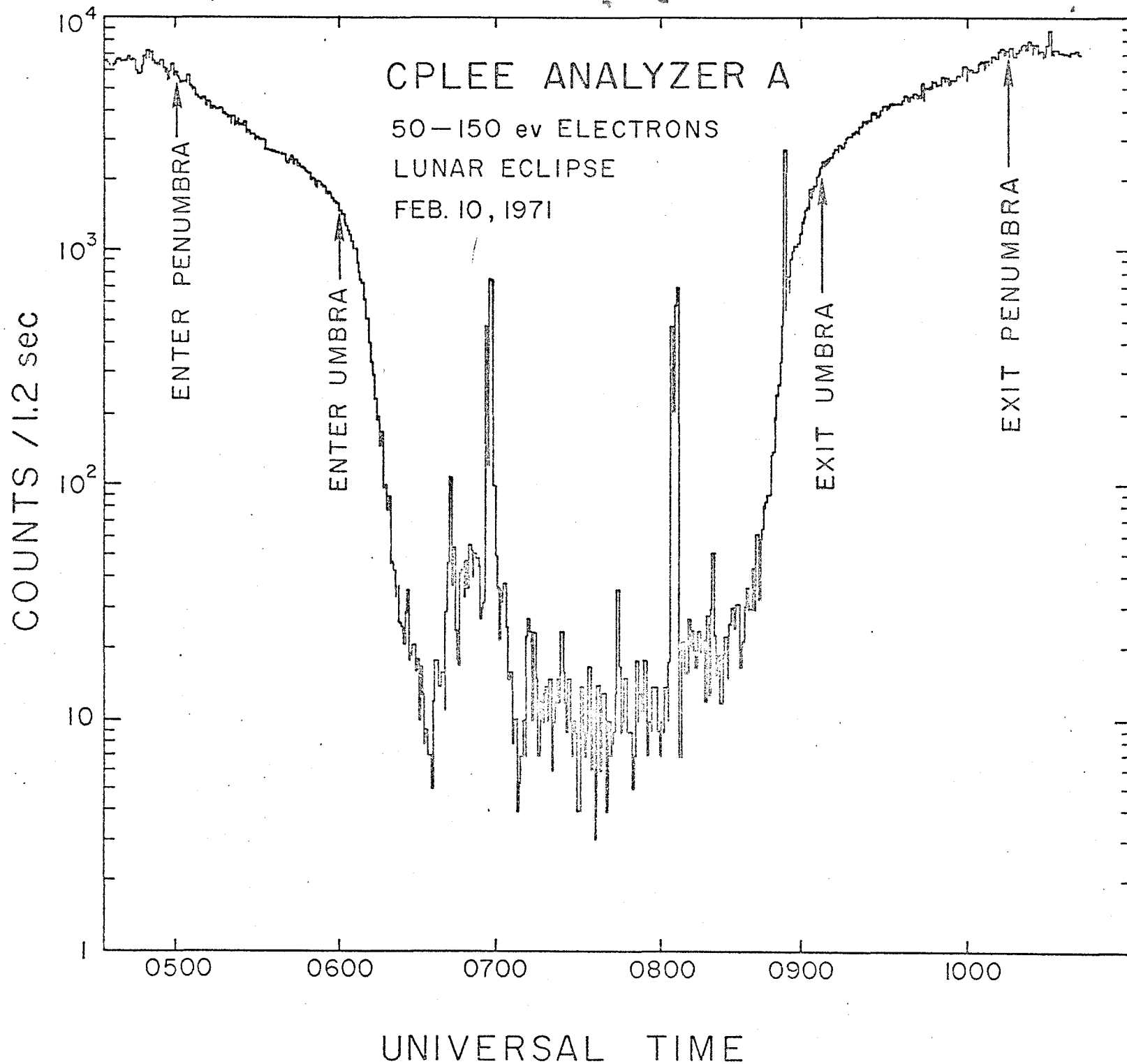


FIGURE 8

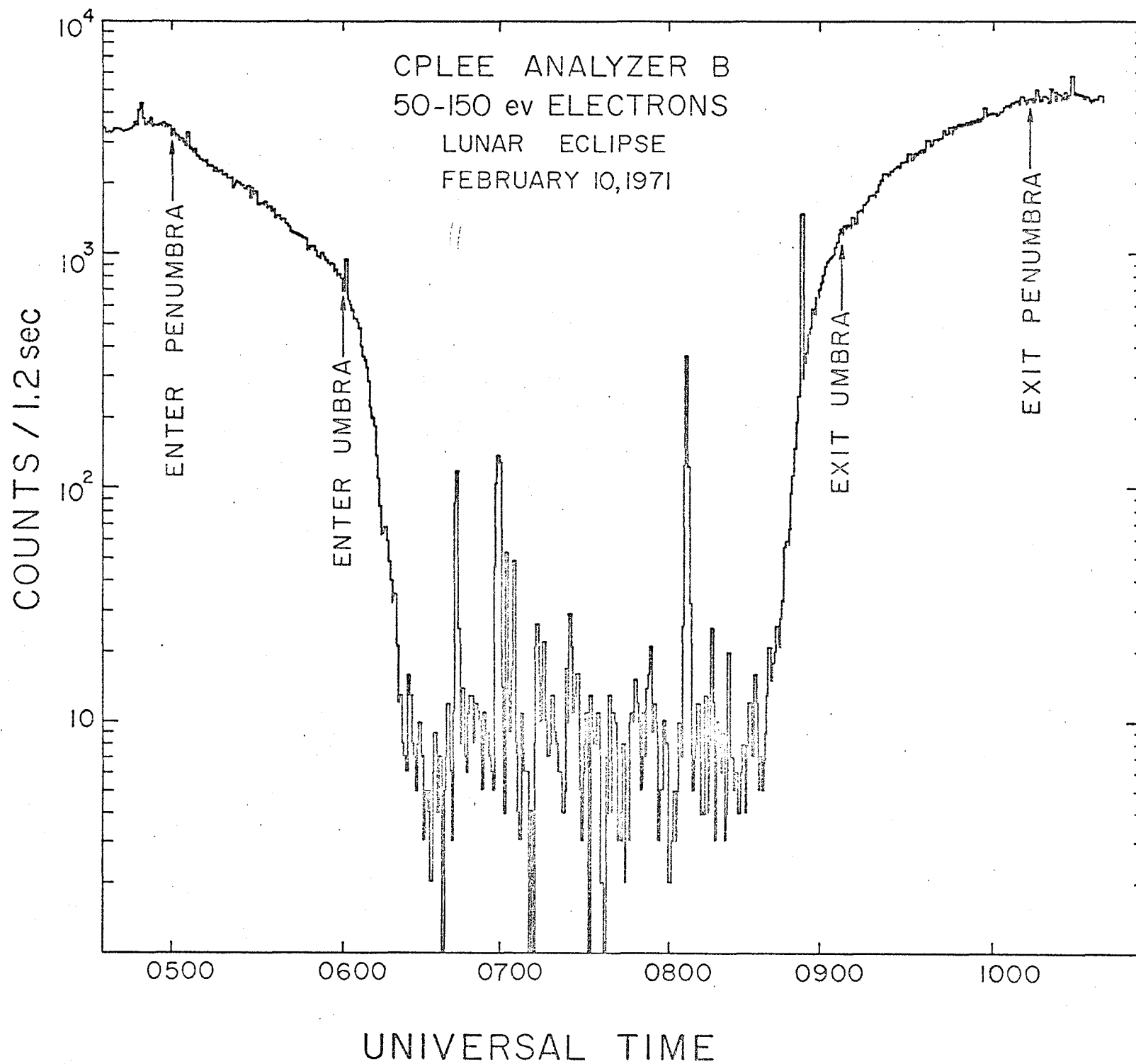


FIGURE 9

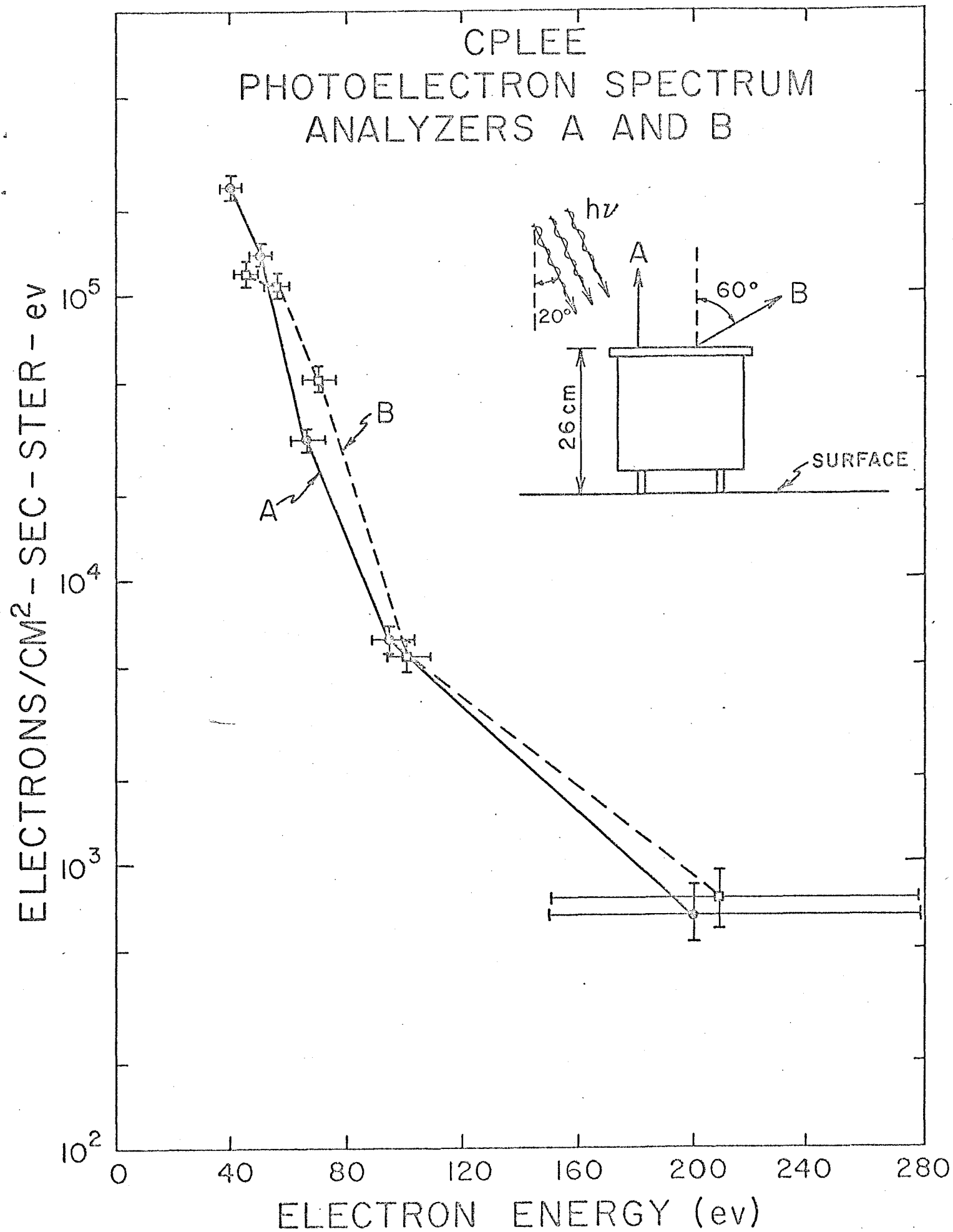


FIGURE 10

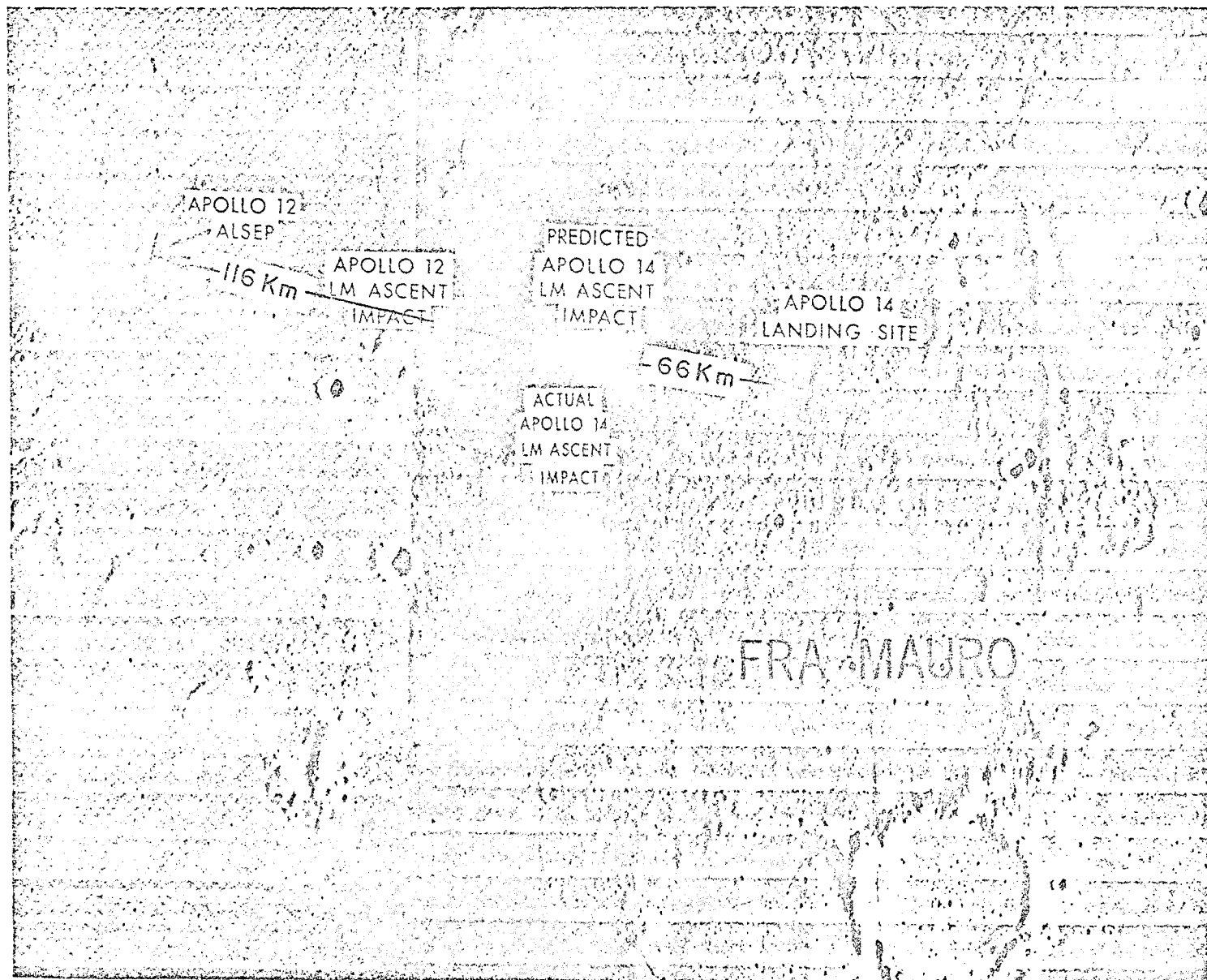


FIGURE 11

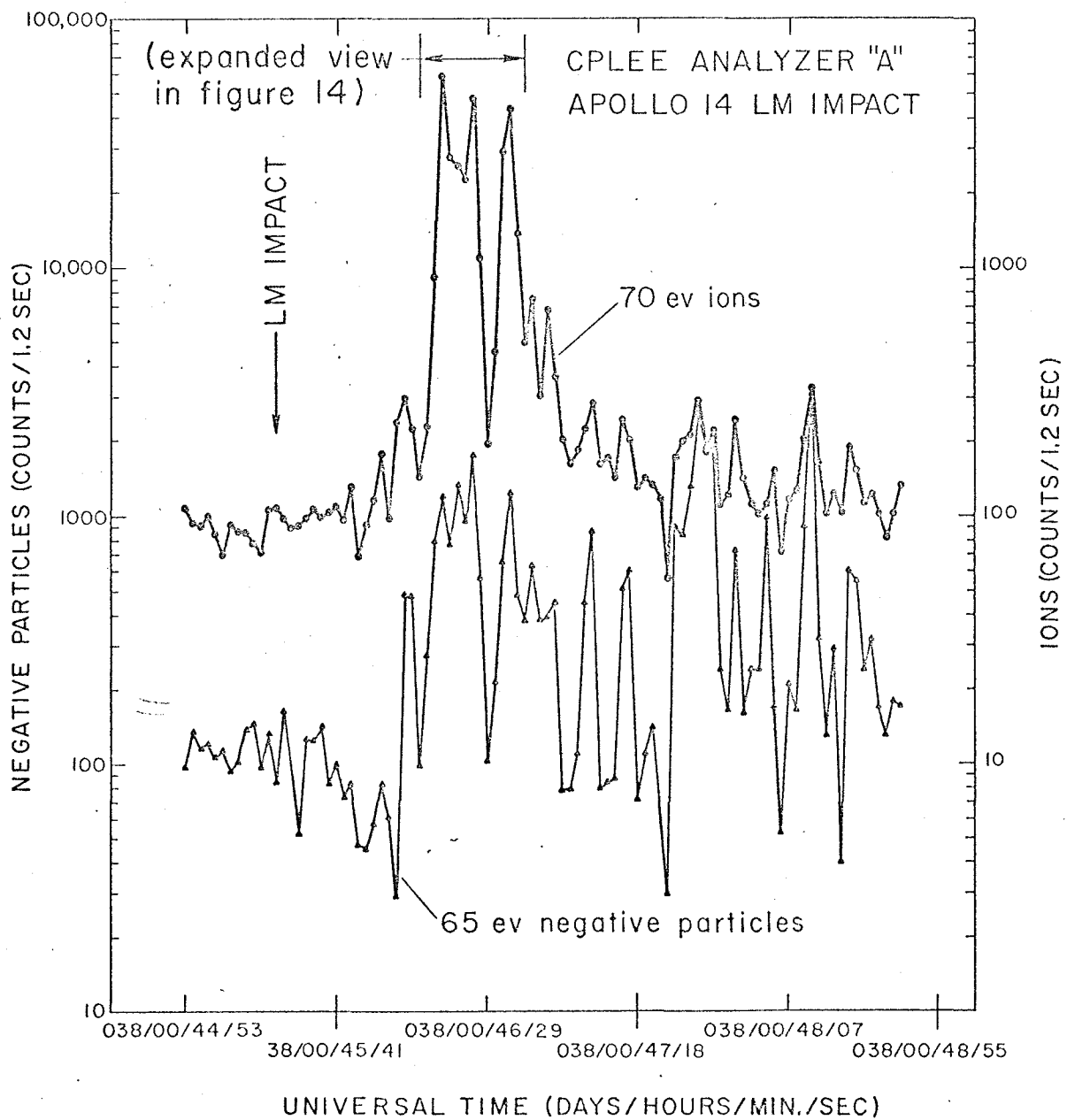


FIGURE 12

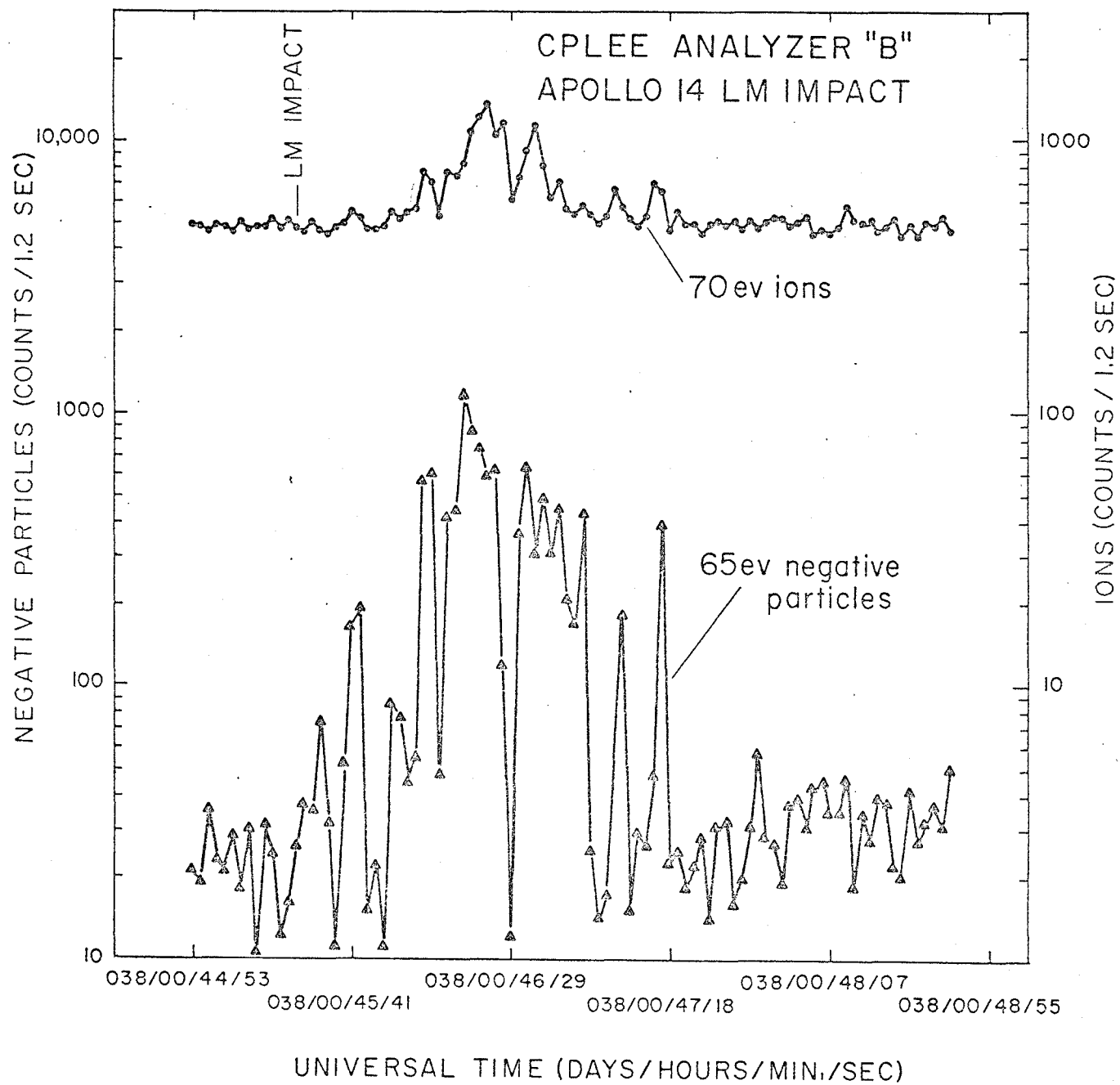


FIGURE 13

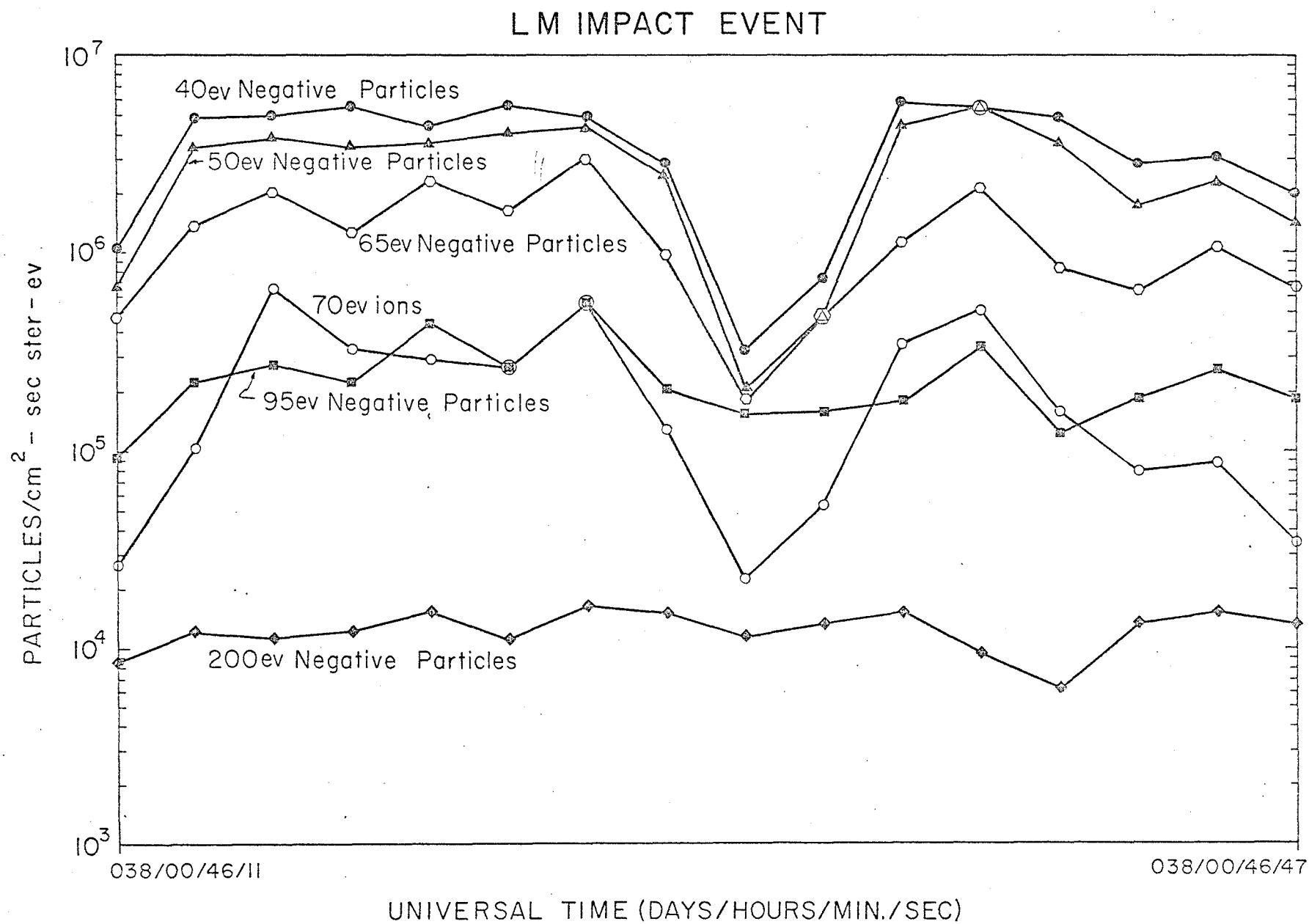


FIGURE 14

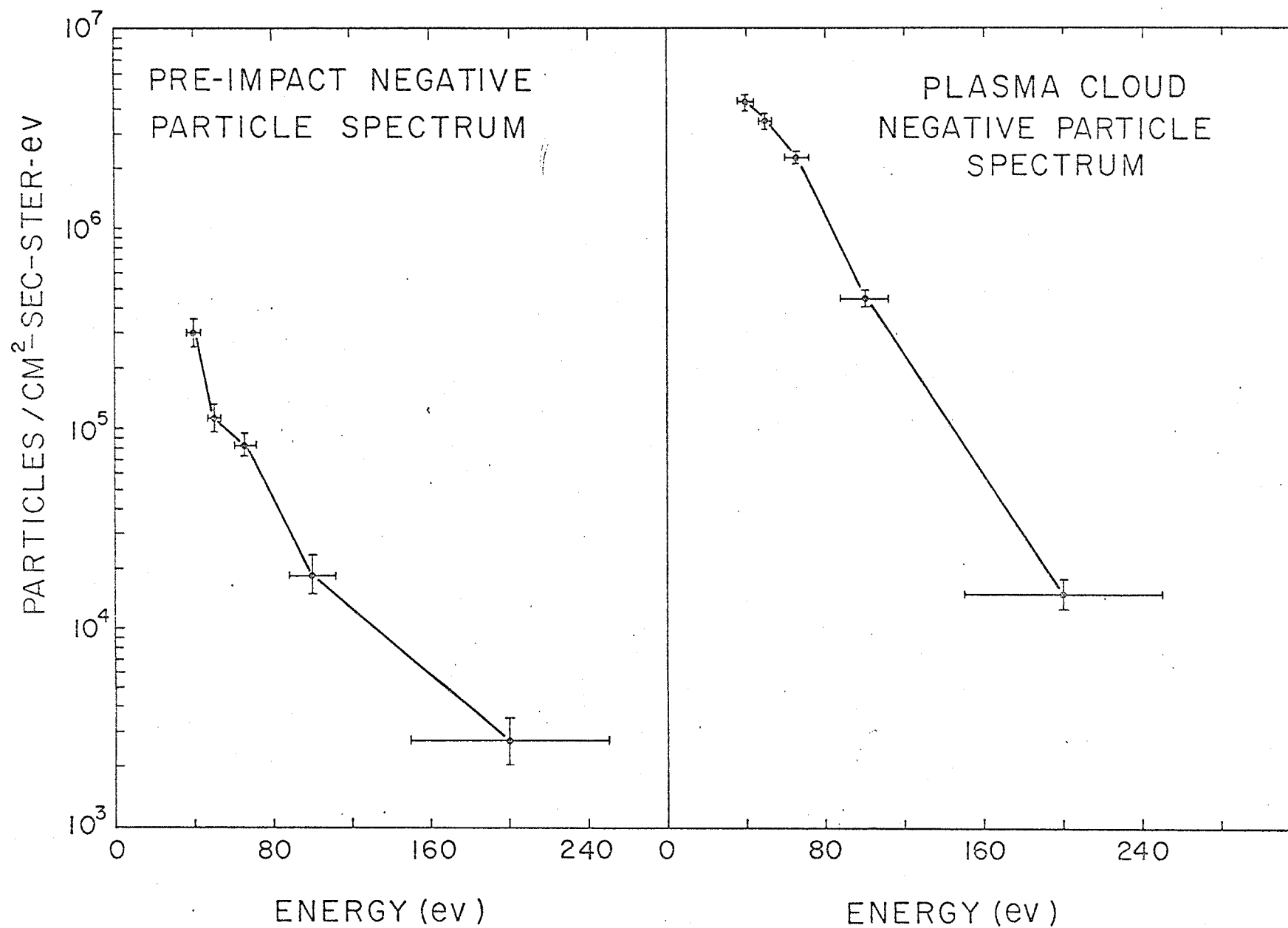


FIGURE 15

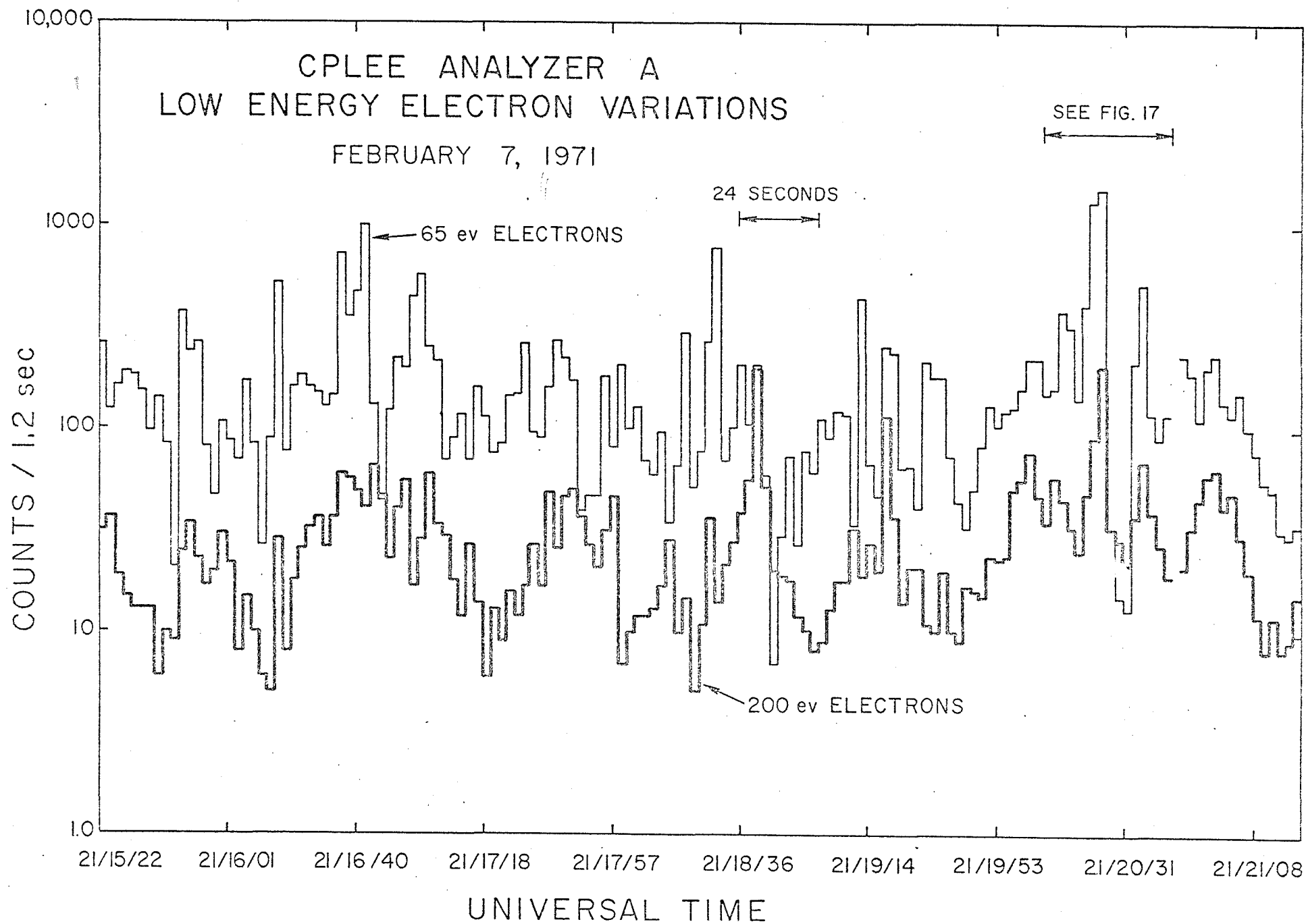


FIGURE 16

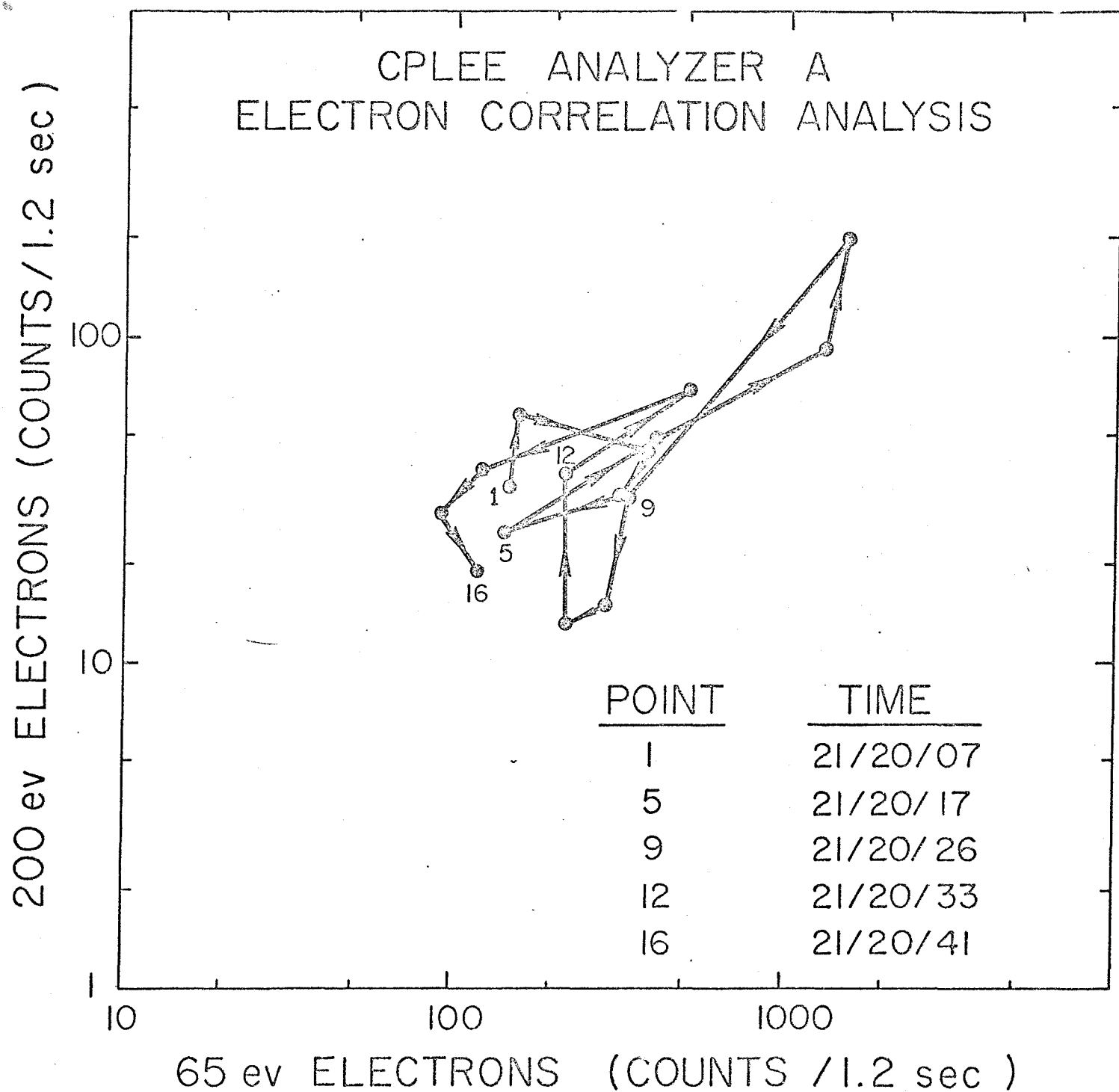


FIGURE 17

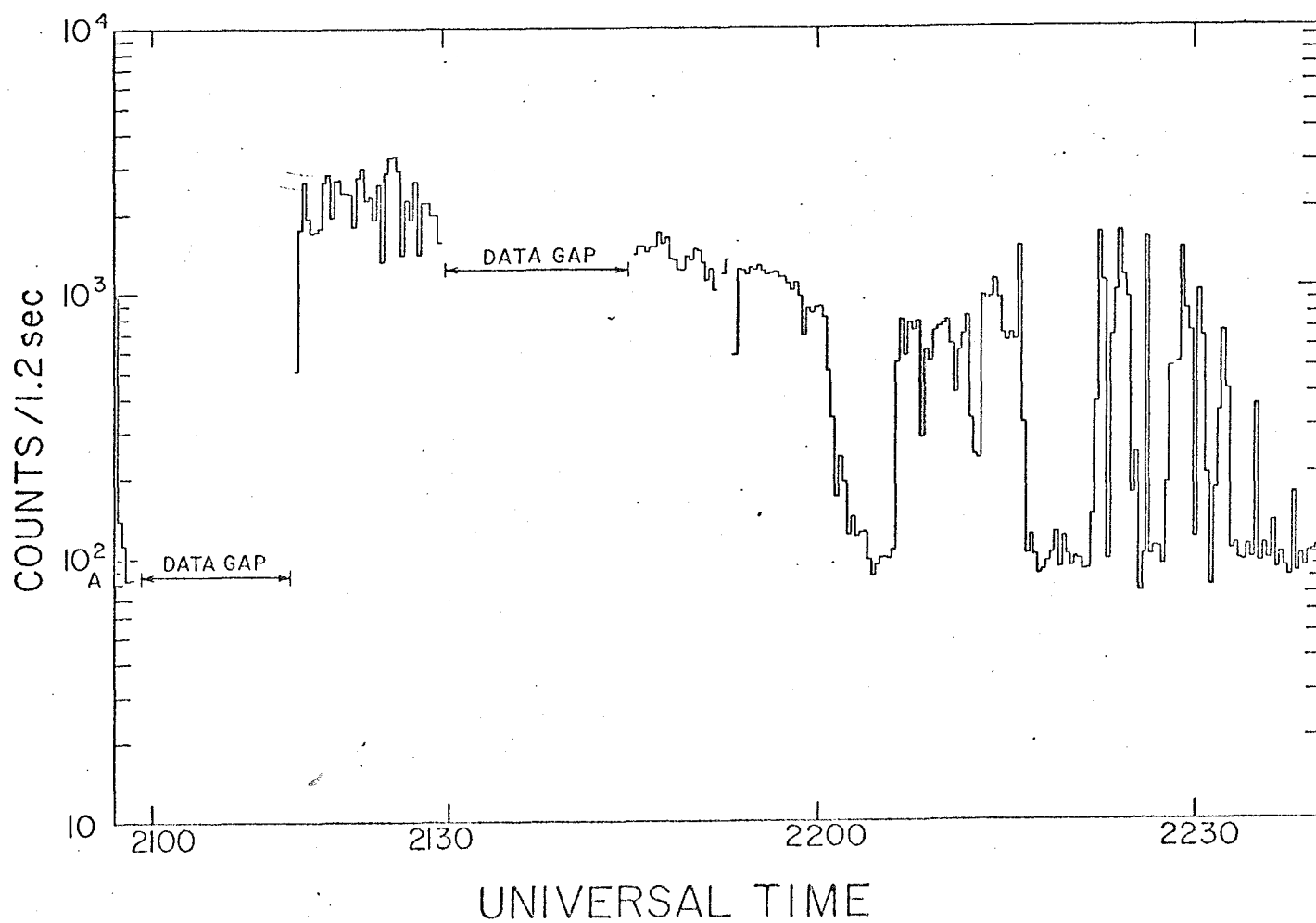
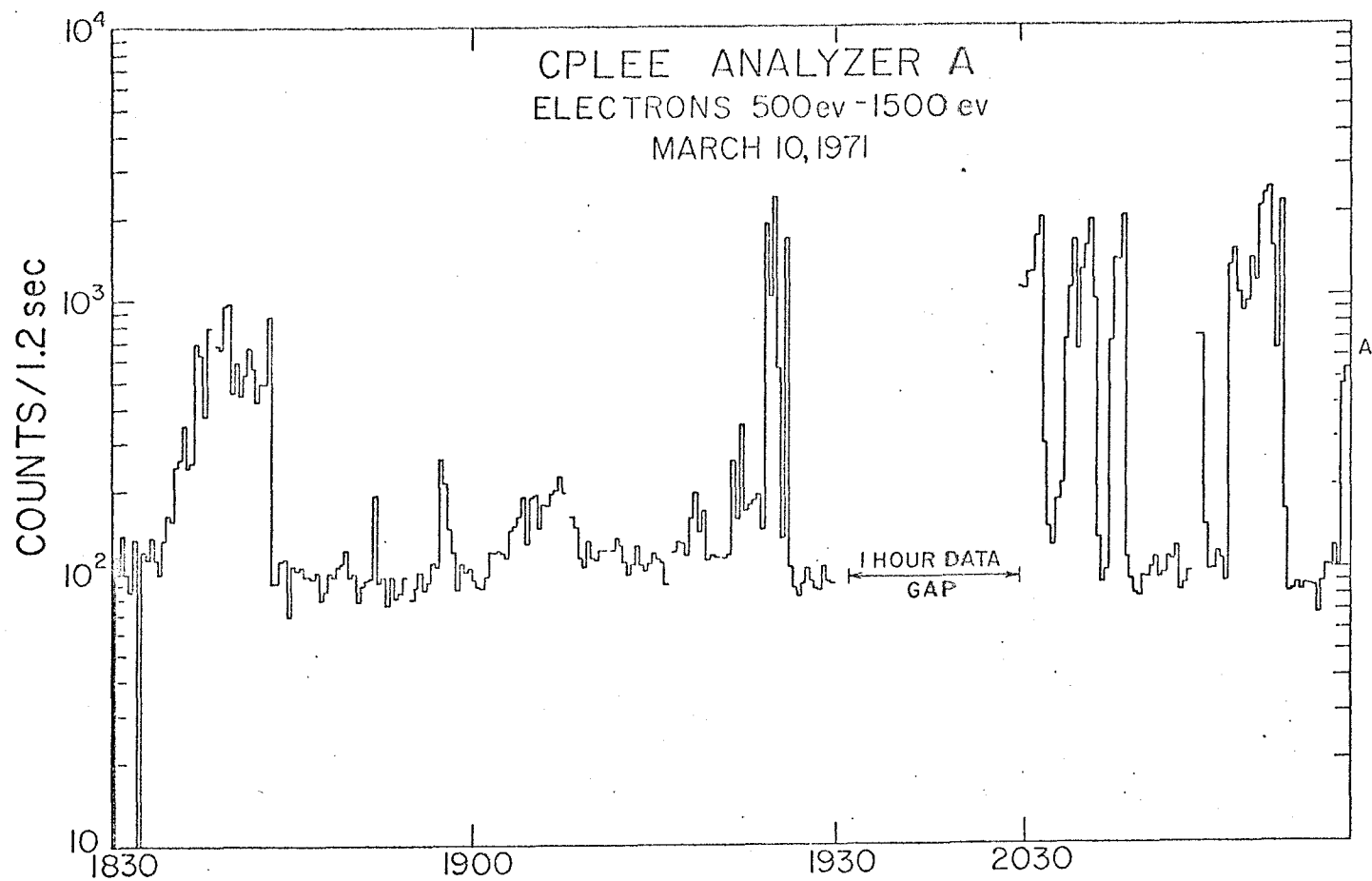


FIGURE 18

Position of CPLEE in the Solar
Magnetospheric Y-Z plane.
March 10 thru March 12, 1971

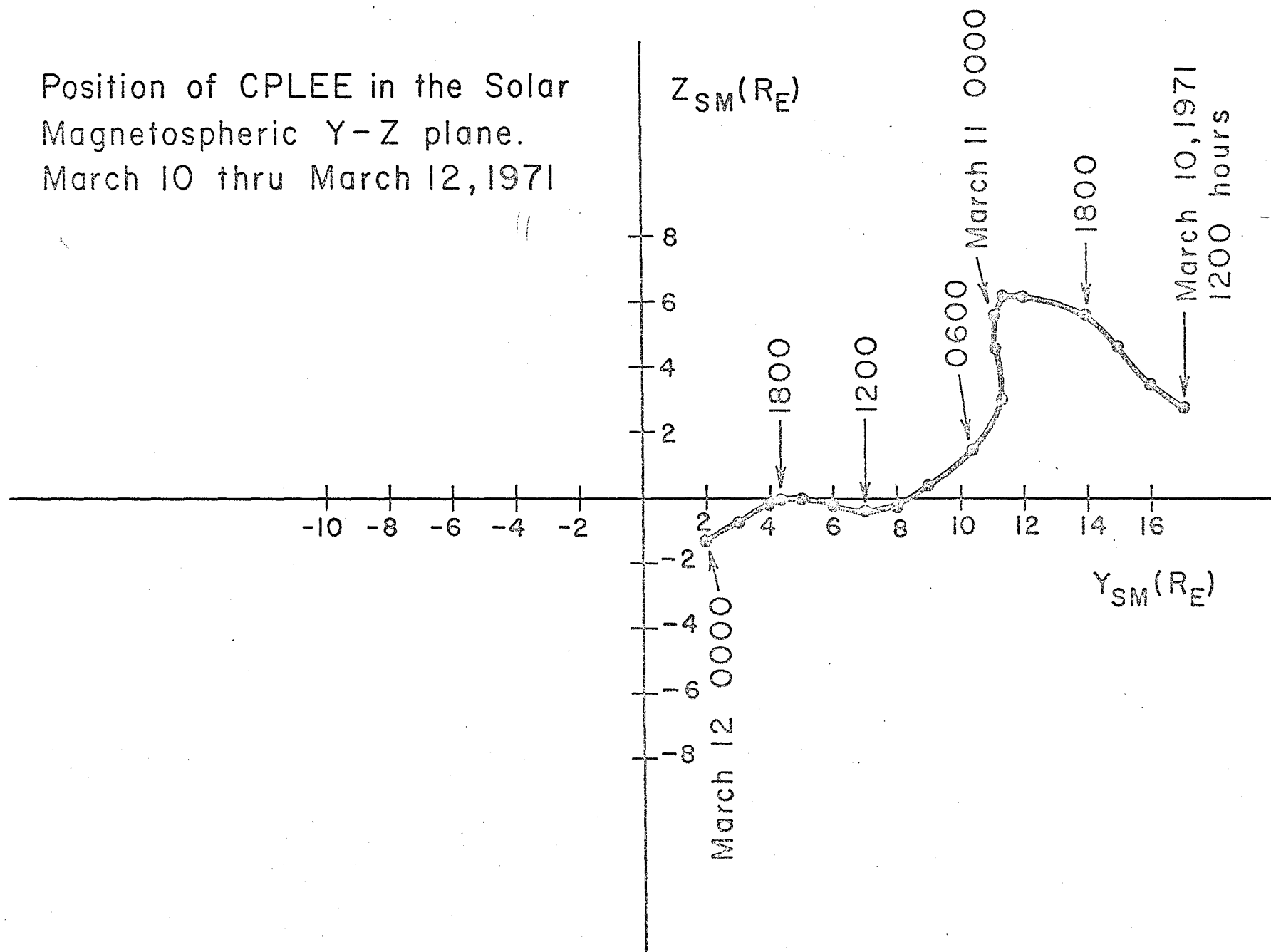


FIGURE 19

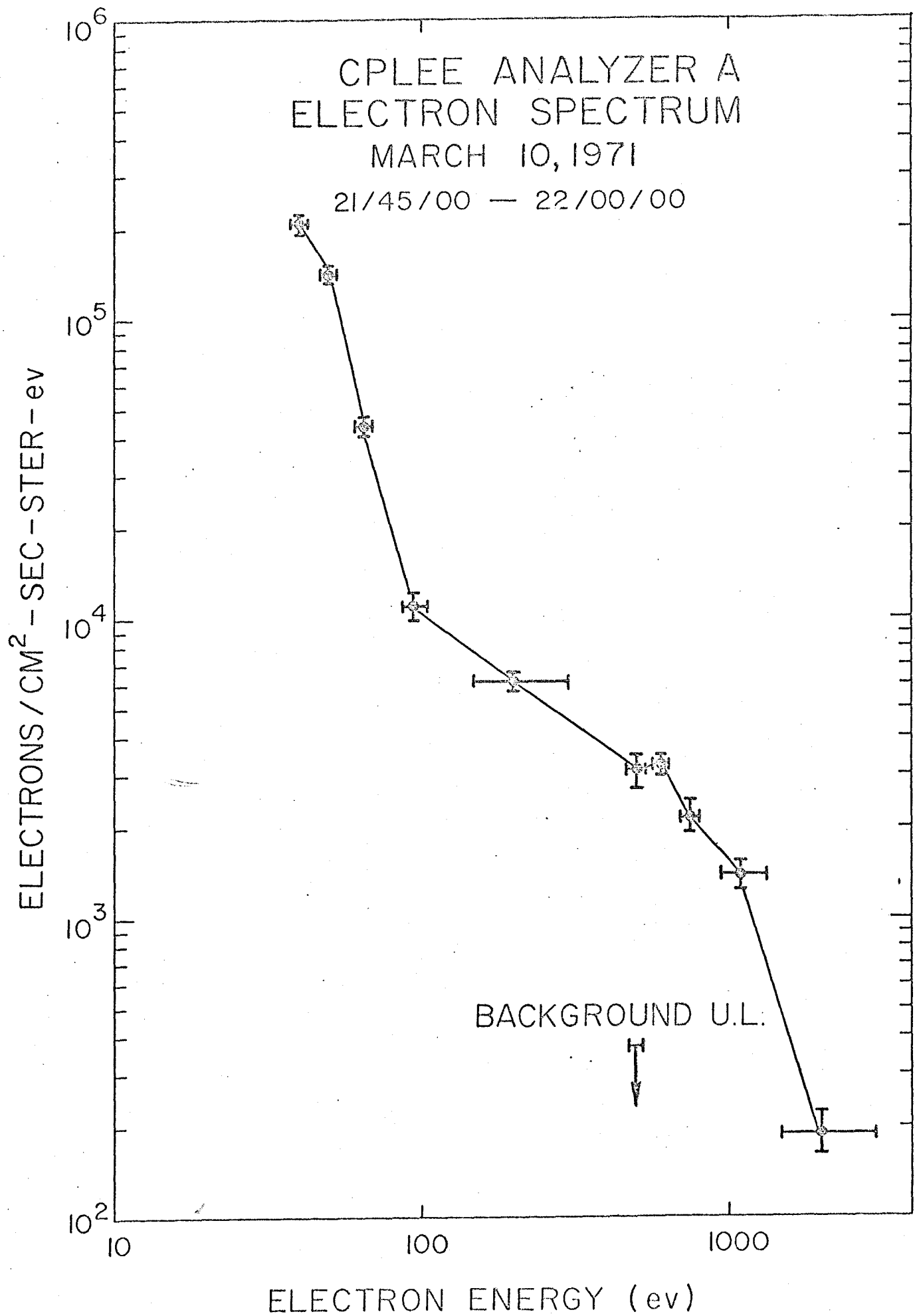


FIGURE 20

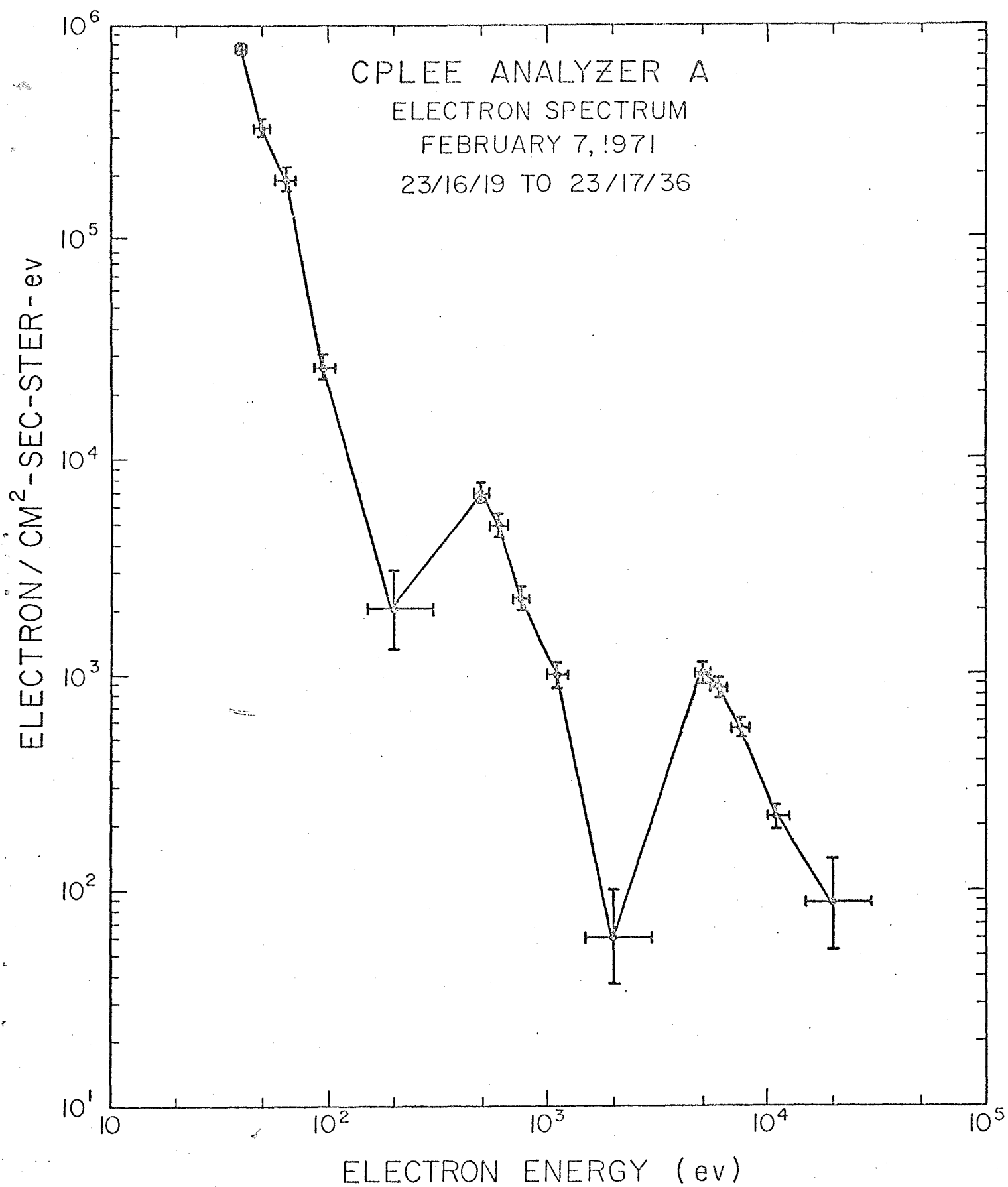


FIGURE 21

TWINS I B
PRECIPITATED AURORAL ELECTRONS

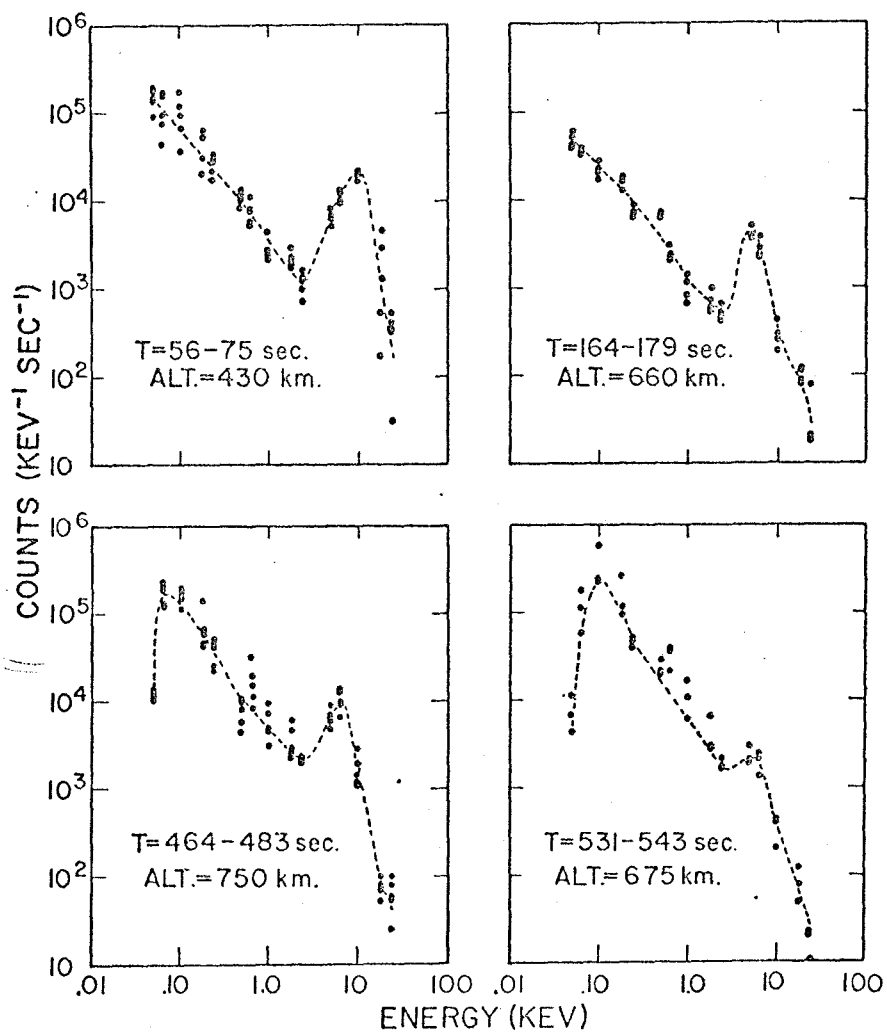


FIGURE 22

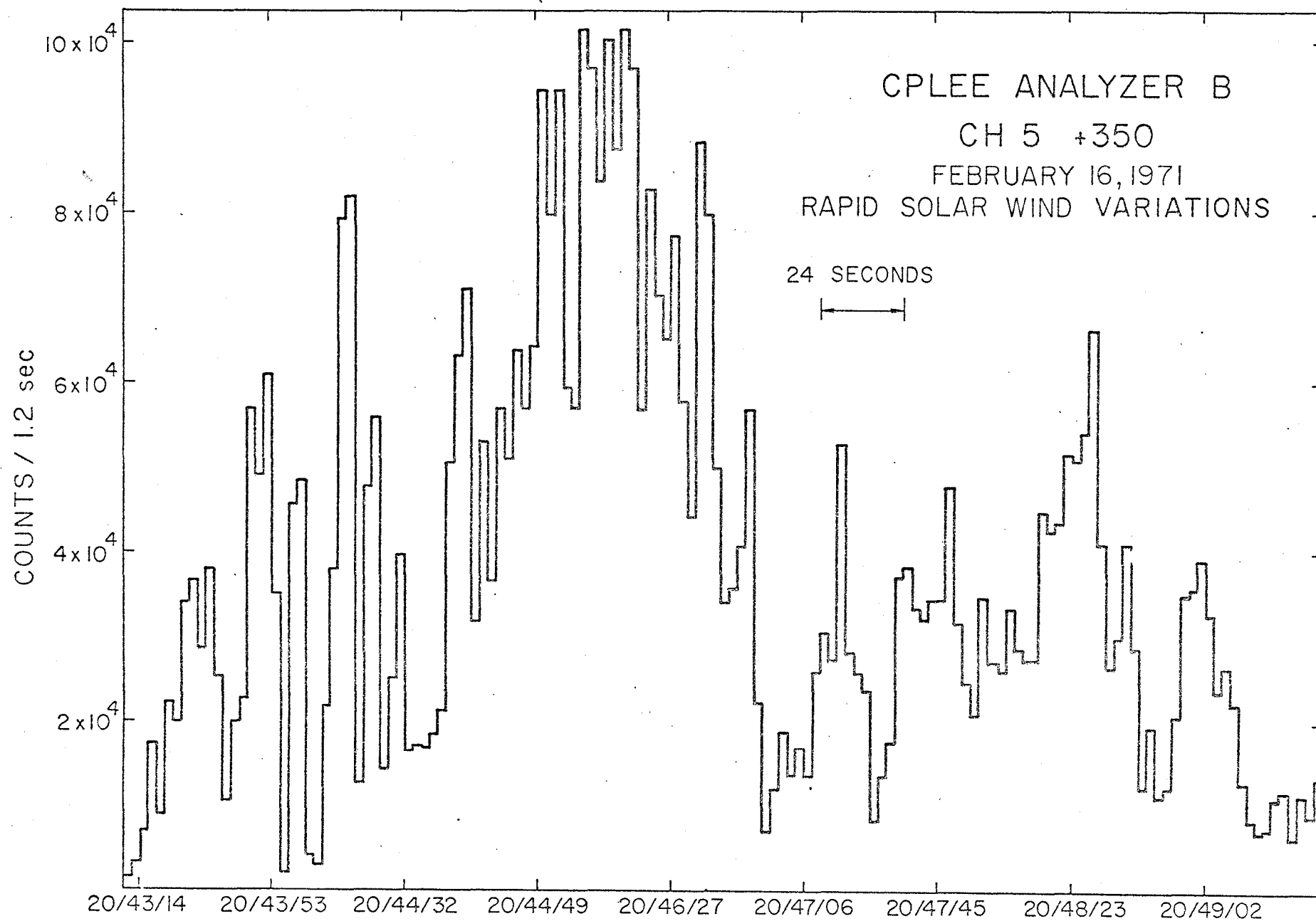


FIGURE 23